



A distributed real-time control algorithm for energy storage sharing

Hailing Zhu*, Khmaies Ouahada

Department of Electrical and Electronic Engineering Science, University of Johannesburg, South Africa



ARTICLE INFO

Article history:

Received 10 October 2019

Revised 15 July 2020

Accepted 10 September 2020

Available online 29 September 2020

Keywords:

Energy management
Lyapunov optimization
Energy storage sharing
Smart grid

ABSTRACT

In this paper, energy storage sharing among a group of cooperative households with integrated renewable generations in a grid-connected microgrid in the presence of dynamic electricity pricing is studied. In such a microgrid, a group of households, who are willing to cooperatively operate a shared energy storage system (ESS) via a central coordinator, aims to minimize their long term time-averaged costs, by jointly taking into account the operational constraints of the shared energy storage, the stochastic solar energy generations and time-varying load requests from all households, as well as the fluctuating electricity prices. We formulate this energy management problem, which comprises storage management and load control, as a constrained stochastic programming problem. Based on the Lyapunov theory, a distributed real-time sharing control algorithm is proposed to provide a suboptimal solution for the constrained stochastic programming problem without requiring any system statistics. The proposed distributed real-time sharing control algorithm, in which each household independently solves a simple convex optimization problem in each time slot, can quickly adapt to the system dynamics. The performance of the proposed low-complexity sharing control algorithm is evaluated via both theoretical analysis and numerical simulations. By comparing with a greedy sharing algorithm and the distributed ESSs case, it is shown that the proposed distributed sharing control algorithm outperforms in terms of both cost saving and renewable energy generation utilization.

© 2020 Elsevier B.V. All rights reserved.

1. Introduction

The fast-growing electric demand coupled with the concern of the carbon dioxide emission of traditional fossil-fuel based electricity generation has motivated a green power system with users deploying distributed renewable energy generators, e.g., wind turbines and solar photovoltaics (PVs). In South Africa, where annual solar radiation ranges from 2400 to 2800kWh/m² [1], a strong solar radiation resource makes solar energy a particularly attractive option. Associated with global solar PV price reductions and spurred on by high annual grid power price increases, solar PV generator installation in South Africa has also been accelerating.

However, the inherently intermittent and stochastic nature of renewable energy production owing to weather variability poses significant challenges to efficient utilization of renewable energy. To address this issue, various techniques have been proposed. For instance, demand response approaches reschedule the electricity loads of users in response to the variation of renewable energy generations and/or electricity prices [2,3]. Nevertheless, demand

response alone may not be sufficient to alleviate the issue, since users have loads that they do not want to be deferred in general.

Increasing dynamics in power systems due to renewable integration and electricity demands have resulted in the exploration of energy storage systems (ESSs) for potential solutions [4] to decouple the time of renewable generation and consumption. From the perspective of power grid operation, the benefits of ESSs including generation backup, transmission support and voltage control have been well-recognized [5]. On the other hand, from the user's perspective, ESSs can be integrated with distributed renewable generations as a more practical solution to improve the energy efficiency and reliability by storing surplus energy generated from renewable resources and cheaper energy at times of lower electricity prices for later use at times of renewable energy generation shortages and/or higher electricity prices.

This work mainly focuses on the interplay between energy supply and energy storage at the user side. There have been many studies on energy management in the context of renewable integration and energy storage from the perspective of demand side management. Most of the previous studies considering energy storage-based demand management assume that each user has its own ESS and analyze the energy storage management problem from a single user point of view. For instance, in recent studies

* Corresponding author.

E-mail addresses: kasha0306@gmail.com (H. Zhu), kouahada@uj.ac.za (K. Ouahada).

Nomenclature

| | | | |
|----------------------|---|--------------------|--|
| $g_{pv,i}(t)$ | energy harvested from household i 's solar PV generator in time slot t | $p(t)$ | unit energy price from the main grid |
| $g_{i,i}(t)$ | energy purchased from the main grid by household i in time slot t that directly supplies the household i 's load | p_{max} | maximum unit energy price from the main grid |
| $g_{s,i}(t)$ | energy purchased from the main grid by household i in time slot t that is stored into the shared battery | p_{min} | minimum unit energy price from the main grid |
| $g_{ch,i}(t)$ | energy charged by household i in time slot t | $s(t)$ | state of charge (SoC) in time slot t |
| $g_{dis,i}(t)$ | energy discharged by household i in time slot t | S_{max} | maximum energy level required in the battery |
| $D_i(t)$ | household i 's serving load in time slot t | S_{min} | minimum energy level required in the battery |
| $\bar{D}_i(t)$ | maximum energy demanded by household i in time slot t | $b_i(t)$ | household i 's effective charging and discharging amount in time slot t |
| $\underline{D}_i(t)$ | minimum energy demanded by household i in time slot t that cannot be shed | R_{ch} | maximum charging rate of the battery |
| $\alpha_i(t)$ | indicator of the sensitivity of household i towards its energy consumption deviation $\bar{D}_i(t) - D_i(t)$ in time slot t | R_{dis} | maximum discharging rate of the battery |
| β_i | upper bound of household i on the long-term time-averaged load shedding ratio | $\zeta_{ch,i}(t)$ | percentage of the maximum charging rate, R_{ch} , taken by household i |
| | | $\zeta_{dis,i}(t)$ | percentage of the maximum discharging rate, R_{dis} , taken by household i |

[6,7], the authors investigated single user optimal charging and discharging policies that balance cost savings with user convenience, such as activity delay, by exploiting the price variations without having to shift user demand to the low-price periods.

In recent years, the concept of ESS sharing, where the surplus renewable energy or cheaper energy of some users can be charged into a shared (common) ESS and then can be discharged by other users, has received increasing attention [8–14]. An ESS shared across a group of users, who can be energy consumers in an industrial park or neighboring households in a community, can benefit users not only through sharing the installation and maintenance costs of the ESS but also by exploiting the non-overlapping power consumption patterns of users. Nevertheless, ESS sharing also brings increasing challenges in energy storage management and load management.

In this paper, we consider a microgrid of a group of households with their individual renewable energy generators, who are willing to share an ESS (in the form of a battery) in a cooperative manner, aiming to minimize their long term energy consumption costs. In this energy storage sharing system, the main challenge of energy management is how to dynamically coordinate the households to optimally utilize the shared ESS, i.e., how to optimally charge/discharge energy to/from the shared ESS, so as to minimize their individual energy consumption costs while satisfying their individual preferences. This energy management problem can be viewed as an energy storage management problem combined with a demand side management problem.

Due to its finite capacity, the shared ESS introduces correlation across time. Specifically, current charging/discharging actions impacted by the previous charging/discharging actions will impact the future charging/discharging actions. Given the inherent time-coupling feature of the ESS, the uncertainties in the multiple renewable generations and power demand requests from different households, as well as the electricity price variations, dynamically coordinating energy storage among a group of households is challenging when integrating energy storage management with demand side management.

Different mechanisms and approaches have been proposed to provide cost savings through a shared ESS. The authors in [8] discussed the energy storage managing method in a distribution network based on evenly dividing energy storage between customers and system operator, but does not optimize the division of energy storage. In [14], the authors proposed a reputation-based central-

ized energy management system (EMS) to jointly schedule households' appliances power consumption and allocate the available energy in the shared battery by considering households' reputations, which depend on the amounts of renewable power they have shared. The proposed EMS runs a day-ahead optimization problem which is formulated as a Mixed Integer Linear Programming. In [15], the authors addressed the cost saving trade-off problem of sharing an ESS among multiple users using a Markovian model and proposed a centralized control policy to dynamically allocate battery capacity among users. The policies for energy storage sharing using a predetermined time-of-use pricing scheme was studied in [16], in which, with a finite horizon formulation, an optimal centralized policy was proposed. In [17], a game theoretic approach was presented with a distributed algorithm to determine each user's energy production and storage a day-ahead. In [18], the authors studied a scenario where an aggregator owns a central storage unit and virtualizes the physical storage into separable virtual storage capacities that can be sold to users to store the energy purchased from the main grid, and modeled the interaction between the aggregator and users in each time slot as a two-stage problem. Assuming that users can perfectly predict their renewable generations and loads, a pricing-based virtual storage sharing scheme among a group of users was proposed and the solutions were characterized based on parametric linear programming under a day-ahead prediction on users' renewable generations and loads.

Most of these existing studies on ESS sharing assume that the users' renewable energy generations and loads are known ahead of time to a central agent, who optimizes the charging/discharging energy of each user, or assume perfect forecasting of the renewable generations, the energy demands and the energy prices, which is practically unachievable. In practice, with unpredictable changes in renewable energy generations and demands, adaptive response to the dynamics of the power system by utilizing the shared ESSs is an important requirement in the time-varying environment of the ESS sharing system.

Due to the time coupling constraints brought by the ESS, the optimization problem for energy management in this ESS sharing system turns out to be a time-coupling problem. Previously, such problems are usually solved using approaches based on Dynamic Programming [19], which not only require full statistical information of the random variables in the problem but also suffer from the "curse of dimensionality" problem [20].

Recently, the Lyapunov optimization theory [21], an effective method to deal with stochastic optimization and stability problems, has been widely adopted in the literature, such as [22–26], to develop online algorithms that require no *a priori* statistical knowledge of the underlying stochastic processes for real-time energy management in microgrids with renewable energy resources combined with ESSs. Using the Lyapunov optimization theory for event-driven queueing systems, an optimization problem with time-coupling constraints can be reformulated to a relaxed problem, which can be solved in each time slot based on the current system state and provides a suboptimal solution for the optimization problem. No information about the future or past system states is required. For instance, in Ref. [22], the optimal cost saving policies using the Lyapunov theory for a single storage system were studied and a real-time control algorithm was proposed to minimize a user’s long term expected energy cost considering a renewable energy generator and a battery. The authors in Ref. [24] proposed a real-time distributed algorithm based on the Lyapunov optimization theory to coordinate a group of distributed storage units to provide power balancing service to a power grid through charging or discharging. The proposed algorithm accommodates a wide spectrum of vital system characteristics, including time-varying power imbalance amount and electricity price, finite battery size constraints, cost of using external energy sources, and battery degradation. However, most of the existing studies primarily consider a single user single ESS scenario or a distributed ESSs scenario.

In this paper, we focus on developing a real-time control algorithm for a battery sharing system. The energy management problem for the ESS sharing system under consideration is first formulated as a constrained stochastic programming problem. The Lyapunov optimization technique is then applied to design a real-time sharing control strategy for storage control and load management for multiple households, which requires no statistical knowledge of the stochastic renewable energy generations, the uncertain power loads and the time-varying electricity prices, so as to minimize the long term energy consumption costs of all households. Then, a distributed battery sharing control algorithm with low computational complexity, in which each household’s energy management optimization problem is solved locally with almost all information obtained locally, is proposed to implement the Lyapunov-based real-time sharing control strategy. Based only on the current system state, the proposed sharing control algorithm coordinates the utilization of the shared battery among the group of households in a distributed manner, by jointly optimizing energy charging/discharging and load management for all households while satisfying each household’s time-varying preference on energy use, and imposes load shedding and renewable energy curtailment if necessary.

The rest of the paper is structured as follows. The system model of a microgrid with a group of households sharing a common ESS is described in Section 2. In Section 3, we formulate the optimization problem for energy management in this sharing system. In Section 4, a distributed real-time sharing control algorithm is proposed based on the Lyapunov theory to solve the optimization problem and its performance is analyzed. Numerical results obtained through simulation evaluations are presented in Section 5. Finally, concluding remarks are provided in Section 6.

Notations: The main symbols used in this paper are summarized in *List of Main Symbols*.

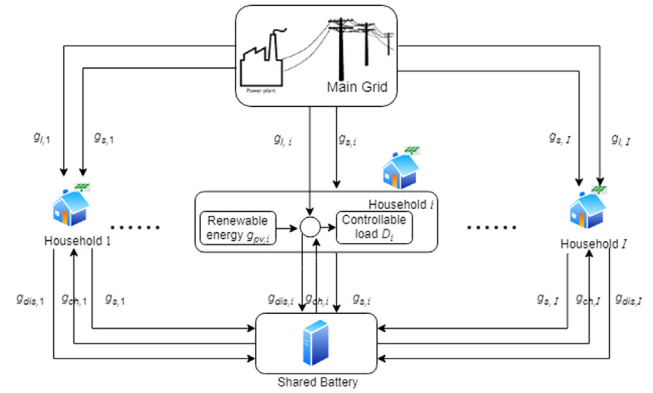


Fig. 1. System Model.

2. System model

We consider a smart community that consists of an energy storage sharing management (ESSM) system for a group of households $\mathcal{H} = \{1, \dots, I\}$ whose load profiles are different and each of whom has an on-site renewable generator (RG). As shown in Fig. 1, the ESSM system contains an energy storage battery with a finite capacity shared among all households who can charge energy harvested from their RG or purchased from the main grid (MG) into the battery. The households’ load demands can be supplied by their individual RGs, the shared energy storage and the MG. In this sharing system, the households cooperatively operate the shared battery via a central coordinator, who manages the shared battery to make sure its operational constraints are satisfied, so as to jointly minimize their electricity consumption costs by utilizing their renewable energy together with the MG combined with the finite-capacity energy storage. We assume that the ESSM system operates in slotted time $t \in \{0, 1, \dots, T - 1\}$.

1) Renewable generator

Each household has a solar PV generator with different capacity and the amount of harvested energy in a time slot varies over time. Let $g_{pv,i}(t)$ denote the energy harvested from household i ’s solar PV generator in time slot t . Since $g_{pv,i}(t)$ is random due to the randomness of the solar source, we assume no prior knowledge of $g_{pv,i}(t)$ or its statistics.

2) Main grid power

Each household can purchase energy from the MG in time slot t at the unit price $p(t)$, $p_{min} \leq p(t) \leq p_{max}$, which is time-varying and only known in time slot t . Let $g_{li}(t)$ denote the amount of energy purchased from the MG by household i in time slot t that directly supplies the household i ’s load, and $g_{si}(t)$ denote the amount of energy purchased from the MG by household i in time slot t that is stored into the shared battery to take advantage of price variations. Then the energy cost of household i in time slot t is

$$C_{MG,i}(t) = [g_{li}(t) + g_{si}(t)]p(t) \quad \forall i \in \mathcal{H}. \quad (1)$$

3) Local power demand

In every time slot, each household decides how much load to consume. The loads of each household can be classified into two categories:

- inelastic loads (in unit of kWh) represent the critical demands such as refrigerator and lights, which should not be shed or shifted over time.
- elastic loads (in unit of kWh) represent the controllable energy requests such as air conditioners and other smart appliances, which can be flexibly curtailed or scheduled over time to minimize costs.

There is great potential to exploit the inherent flexibility of such elastic loads. We consider a demand side management in the microgrid, where flexible loads can be shed in response to supply conditions. For household i , its demand $D_i(t)$ in time slot t is bounded by:

$$\bar{D}_i(t) \geq D_i(t) \geq \underline{D}_i(t) \quad \forall i \in \mathcal{I}, \quad (2)$$

where $\bar{D}_i(t)$ is the maximum energy demanded by household i in time slot t , i.e., the most preferred energy consumption of household i , and $\underline{D}_i(t)$ is the minimum energy demanded by household i in time slot t that cannot be shed, i.e., the inelastic loads. Note that $\bar{D}_i(t)$ and $\underline{D}_i(t)$ are the demand requests decided by households based on the physical constraints and their willingness to shed their elastic loads. If a household refuses load shedding, the requested maximum and minimum energy will be the same. The demand requests of each household in each time slot are assumed to be stochastic and private information.

However, load shedding used for cost saving may cause discomfort to the households. When the shed energy consumption $D_i(t)$ deviates from the preferred energy consumption $\bar{D}_i(t)$, discomfort experienced by household i can be represented by a discomfort cost function

$$C_{COM,i}(t) = \alpha_i(t) \left[\bar{D}_i(t) - D_i(t) \right]^2 \quad \forall i \in \mathcal{I}, \quad (3)$$

where the weighted coefficient $\alpha_i(t)$ is a positive constant used to indicate the sensitivity of household i towards the energy consumption deviation $\bar{D}_i(t) - D_i(t)$: the higher the value of $\alpha_i(t)$, the more sensitive the household i towards the energy consumption deviation.

Meanwhile, in order to control the quality-of-service (QoS) [25] for the households, an upper bound is imposed on the portion of the unsatisfied flexible load, which can be formally expressed by [27]

$$\lim_{T \rightarrow \infty} \frac{1}{T} \sum_{t=0}^{T-1} \left[\frac{\bar{D}_i(t) - D_i(t)}{\bar{D}_i(t) - \underline{D}_i(t)} \right] \leq \beta_i \quad \forall i \in \mathcal{I}, \quad (4)$$

where $\bar{D}_i(t) - D_i(t)$ is the shed demand, $\bar{D}_i(t) - \underline{D}_i(t)$ is the total demand that can be shed in time slot t , and $\beta_i \in (0, 1]$ is a pre-designed threshold used to control the QoS, i.e., the long-term time-averaged load shedding ratio. It reflects the tolerance of household i to the energy consumption deviation. A smaller β_i indicates a tighter QoS control. Note that both $\alpha_i(t)$ and β_i are decided by household i based on its energy consumption preference and $\alpha_i(t)$ could vary over time in a stochastic manner. In addition, both $\alpha_i(t)$ and β_i are assumed to be private information to household i .

Let $g_{ch,i}(t)$ and $g_{dis,i}(t)$ denote the amount of energy charged and discharged by household i in time slot t , respectively. We assume a priority of using energy harvested from solar PV generator

$g_{pv,i}(t)$ to directly supply $D_i(t)$ and the excessive portion, if any, will be charged into the shared battery. When $D_i(t) \leq g_{pv,i}(t)$, which results in energy surplus, we denote the energy that household i charges into the shared battery in time slot t by

$$g_{ch,i}(t) \leq g_{pv,i}(t) - D_i(t) \quad \forall i \in \mathcal{I}. \quad (5)$$

Note that, since the storage space of the shared battery is limited, not all the excessive portion can be charged into the battery if there is not enough storage space in the shared battery.

When $D_i(t) > g_{pv,i}(t)$, which results in energy deficit, the residual $D_i(t) - g_{pv,i}(t)$ can be served with the energy purchased from the MG $g_{i,i}(t)$ or the energy drawn from the shared battery $g_{dis,i}(t)$. A balance between purchasing the energy from the MG and drawing the energy from the battery must be struck under the following feasibility condition:

$$g_{i,i}(t) + g_{dis,i}(t) = D_i(t) - g_{pv,i}(t) \quad \forall i \in \mathcal{I}. \quad (6)$$

It is noticed that, $g_{dis,i}(t) = 0$ in case of energy deficit and $g_{ch,i}(t) = 0$ in case of energy surplus. Since energy surplus and energy deficit can not happen at the same time, we have

$$g_{ch,i}(t)g_{dis,i}(t) = 0 \quad \forall i \in \mathcal{I}. \quad (7)$$

4) Shared Energy Storage

The shared battery has a finite storage capacity S_{cap} . In practice, batteries are not ideal. There are energy conversion losses during the charging and discharging processes. Let $\eta_{ch} \in (0, 1]$ and $\eta_{dis} \in [1, \infty)$ be the charging and discharging efficiency coefficient, respectively.

a) Denote $s(t)$ as the energy state of the battery at the beginning of time slot t . The energy state $s(t)$, known as state of charge (SoC), in kWh, fluctuates over time and evolves as follows:

$$s(t) = s(t-1) + \eta_{ch} \sum_{i \in \mathcal{I}} [g_{ch,i}(t) + g_{s,i}(t)] - \eta_{dis} \sum_{i \in \mathcal{I}} g_{dis,i}(t) \\ \triangleq s(t-1) + \sum_{i \in \mathcal{I}} b_i(t) \quad \forall i \in \mathcal{I}, \quad (8)$$

where $b_i(t)$ is defined as the effective charging and discharging amount in time slot t . We assume that there is no self-discharging.

b) Because of limitation imposed by the charging and discharging circuits, the amounts of energy charged into and discharged from the battery are upper bounded. Denote the maximum charging and discharging rate of the battery by R_{ch} and R_{dis} , respectively, so that

$$0 \leq \sum_{i \in \mathcal{I}} [g_{ch,i}(t) + g_{s,i}(t)] \leq R_{ch} \\ 0 \leq \sum_{i \in \mathcal{I}} g_{dis,i}(t) \leq R_{dis} \quad \forall i \in \mathcal{I}. \quad (9)$$

c) To reduce the impact of degradation, the operation of energy storage system should be controlled to increase its benefit at least cost. Charging a battery near its capacity or discharging it close to the zero energy state can significantly reduce battery lifetime [28]. Hence, lower and upper bounds on the battery energy state are usually imposed by its manufacturer or owner. Denote $[S_{min}, S_{max}]$ as the preferred energy range with $0 < S_{min} < S_{max} < S_{cap}$. Then the level of the shared battery in time slot t is bounded by

$$S_{min} \leq s(t) \leq S_{max}. \quad (10)$$

d) Combining (8)–(10), the boundaries of charging and discharging energy in time slot t can be compactly represented as

$$\begin{aligned} 0 &\leq \sum_{i \in \mathcal{J}} [g_{ch,i}(t) + g_{s,i}(t)] \leq \min \left\{ R_{ch}, \frac{S_{max} - s(t-1)}{\eta_{ch}} \right\} \\ 0 &\leq \sum_{i \in \mathcal{J}} g_{dis,i}(t) \leq \min \left\{ R_{dis}, \frac{s(t-1) - S_{min}}{\eta_{dis}} \right\} \quad \forall i \in \mathcal{J}. \end{aligned} \quad (11)$$

The space-availability constraint and the energy-availability constraint in (11) must be satisfied at all time for the charging and discharging decisions to be feasible. In other words, the energy charged/discharged into/from the shared battery must not exceed the storage space/energy available for charging/discharging.

3. Problem statement and formulation

3.1. Problem statement

Solar energy generations of multiple households bring more uncertainties to the energy management problem, making it challenging to balance supply and demand in real-time. In this paper, we study the problem of real-time energy storage and management in this microgrid aiming at achieving the long-term energy consumption objectives of the households while ensuring an acceptable level of the discomfort experienced by each household in real-time, taking into consideration the dynamics of the energy demands, renewable sources and energy prices as well as the operational constraints of the shared battery. In other words, the objective of the ESSM system is to jointly determine energy consumption, energy purchasing and energy charging/discharging actions of all households so as to minimize the long-term time-averaged costs of all households, subject to the operational constraints of the shared battery as well as time-varying solar energy generations from households, in the presence of dynamic electricity prices. Therefore, the control problem can be stated as follows: given the current random renewable supplies, the battery energy level, the energy demand preferences of households and the electricity price, design a control strategy that chooses the energy purchasing vectors, the battery charging and discharging vectors, as well as serving load vectors for all households such that the long-term time-averaged energy consumption costs of all households are minimized.

For the sake of clarity and ease of reading, we define the system state $\mathbf{X}(t)$ in time slot t using the renewable generations and demand preferences of households, the energy price from the MG and the energy state of the shared battery

$$\mathbf{X}(t) \triangleq [\mathbf{g}_{pv}(t), \mathbf{d}(t), p(t), s(t)], \quad (12)$$

where $\mathbf{d}(t) \triangleq [\bar{D}_i(t), \underline{D}_i(t)] \forall i$ is the demand preference vector and $\mathbf{g}_{pv}(t) \triangleq [g_{pv,i}(t)] \forall i$ is the renewable generation vector. We assume that $\mathbf{X}(t)$ is stochastic.

The control vector in time slot t is defined by

$$\mathbf{Y}(t) \triangleq [\mathbf{g}_i(t), \mathbf{g}_s(t), \mathbf{g}_{ch}(t), \mathbf{g}_{dis}(t), \mathbf{D}(t)], \quad (13)$$

where $\mathbf{g}_i(t) \triangleq [g_{l,i}(t)] \forall i$ and $\mathbf{g}_s(t) \triangleq [g_{s,i}(t)] \forall i$ are the energy purchasing vectors for load serving and battery charging respectively, $\mathbf{g}_{ch}(t) \triangleq [g_{ch,i}(t)] \forall i$ and $\mathbf{g}_{dis}(t) \triangleq [g_{dis,i}(t)] \forall i$ are the battery charging

and discharging vectors, respectively, and $\mathbf{D}(t) \triangleq [D_i(t)] \forall i$ is the serving load vector.

With the known information, i.e., the current system state $\mathbf{X}(t)$, the objective of the ESSM system is to make control decision to choose $\mathbf{Y}(t)$ in reaction to the current system state $\mathbf{X}(t)$ in each time slot in order to minimize the households' energy consumption costs, comprising the discomfort costs of load shedding and the costs of energy purchased from the MG, over a long-term T -slot period, while guaranteeing the QoS for each household, by jointly managing energy consumption, supply and storage given the finite battery capacity. We define the instantaneous cost of all households by

$$\begin{aligned} C_{ToT}(t) &= \sum_{i \in \mathcal{J}} C_{MG,i}(t) + \sum_{i \in \mathcal{J}} C_{COM,i}(t) = \sum_{i \in \mathcal{J}} [g_{l,i}(t) + g_{s,i}(t)] p(t) \\ &\quad + \sum_{i \in \mathcal{J}} \alpha_i(t) \left[\bar{D}_i(t) - D_i(t) \right]^2. \end{aligned} \quad (14)$$

Thus, the stochastic control optimization problem of the real-time energy management, called **P1**, can be formulated by

$$\begin{aligned} \mathbf{P1} : \quad &\min_{\mathbf{Y}(t)} \quad \lim_{T \rightarrow \infty} \frac{1}{T} \sum_{t=0}^{T-1} \mathbb{E}\{C_{ToT}(t)\}, \\ &\text{s.t.} \quad (2)(4)(5)(6)(7)(9)(10), \end{aligned} \quad (15)$$

where $\mathbb{E}\{\cdot\}$ is taken with respect to $\mathbf{X}(t)$. Taking the randomness of the system state $\mathbf{X}(t)$ and the random control decision $\mathbf{Y}(t)$ in each time slot into account in the expectations of the objective function and constraints, **P1** seeks control decisions for the entire time horizon up till infinity taking the system dynamics into consideration. However, due to the time-coupling dynamics of (8), the current control action impacted by the previous control actions will impact the future control actions. Therefore, it is challenging to solve the stochastic optimization problem **P1** with the correlated control actions $\mathbf{Y}(t)$ over time.

The optimization problem **P1** can be solved using approaches based on Dynamic Programming [20], provided that the system statistics, e.g., the distributions of the components of $\mathbf{X}(t)$, are known, which might be practically infeasible. In this study, given the stochastic system state $\mathbf{X}(t)$, we are interested in real-time energy management that requires no system statistics while quickly adapting to the system dynamics. Motivated by the recent studies, a real-time algorithm is developed to determine real-time control vector $\mathbf{Y}(t)$ over time, applying the general framework of Lyapunov optimization [21] to reformulate the optimization problem **P1** to handle the time-coupling constraint (10).

3.2. Problem Modification

Time-averaged constraints can be transformed into queue stability constraints and simple real-time algorithms can be provided for complex dynamic systems using the Lyapunov optimization theory. Unfortunately, the time-coupling dynamics of $s(t)$ over time in (8) and the battery capacity constraint in (10), which require that no energy underflow and overflow happen for all time, impose a hard constraint on the charging and discharging decisions in each time slot. As a result, the charging and discharging decisions are correlated with each other over time. Therefore, **P1** cannot be directly solved using the standard Lyapunov optimization techniques. To avoid such coupling, the hard constraint (10) in **P1** is relaxed to a softer constraint, which reflects the long-term time-averaged relationship among the charging and discharging decisions, given by

$$\lim_{T \rightarrow \infty} \frac{1}{T} \sum_{t=0}^{T-1} \mathbb{E} \left\{ \sum_{i \in \mathcal{J}} b_i(t) \right\} = 0. \quad (16)$$

The derivation of (16) is as follows: summing both sides of the energy state Eq. (8) over $t = \{0, 1, \dots, T-1\}$ and dividing them by T yields

$$\frac{1}{T} \sum_{t=0}^{T-1} \sum_{i \in \mathcal{J}} b_i(t) = \frac{s(T-1)}{T} - \frac{s(0)}{T}, \quad (17)$$

where $\sum_{i \in \mathcal{J}} b_i(t)$ is defined as the effective charging and discharging amount in time slot t in (8). Taking expectations on both sides of (17) and taking limits over T to infinity gives

$$\lim_{T \rightarrow \infty} \frac{1}{T} \sum_{t=0}^{T-1} \mathbb{E} \left\{ \sum_{i \in \mathcal{J}} b_i(t) \right\} = \lim_{T \rightarrow \infty} \frac{s(T-1)}{T} - \lim_{T \rightarrow \infty} \frac{s(0)}{T}. \quad (18)$$

Since both $s(T-1)$ and $s(0)$ are finite due to (8), the right hand side of (18) is equal to zero.

The softer constraint in (16) requires that the mean rate of the effective charging and discharging amounts in the whole process is kept stable, instead of bounding the energy state in each time slot in (10). Replacing the time-coupling constraint (10) with the time average queuing constraint (16), we relax **P1** to the following problem:

$$\begin{aligned} \mathbf{P2} : \quad & \min_{\mathbf{Y}(t)} \quad \lim_{T \rightarrow \infty} \frac{1}{T} \sum_{t=0}^{T-1} \mathbb{E} \{ C_{ToT}(t) \}, \\ & \text{s.t.} \quad (2)(4)(5)(6)(7)(9)(16). \end{aligned} \quad (19)$$

Through the relaxation transformation, the dependency of per time slot charging/discharging amount on the battery state $s(t)$ in constraints (10) is removed. Now the standard Lyapunov optimization techniques can be applied to obtain the optimal solution of the relaxed problem **P2** in a way that is independent of battery SoC level. This relaxation technique used to accommodate the type of time-coupling constraints such as (10) was first introduced in [29] for energy management in a data center equipped with an ideal battery, and then was widely adopted in the literature regarding energy storage management. However, with the relaxed constraint (16), the solution to **P2** may not be feasible to **P1**. Hence, in the next section, we present a real-time control algorithm that can guarantee all constraints of **P1** are satisfied. We will show later in Section 4.3 that the solution to **P2** obtained by the proposed real-time algorithm in fact also satisfies (10), so it is feasible for **P1**.

4. Lyapunov-based distributed real-time sharing control algorithm

In this section, we present a real-time sharing control algorithm using the Lyapunov optimization techniques to solve **P2** and provide simple online solutions based on the current information of the system state.

4.1. Virtual queue design

According to the concept of virtual queues from the Lyapunov optimization [21], we first introduce virtual queues to transform the time-averaged inequality and equality constraints (4) and (16) in **P2** into queue stability constraints.

- **Battery Queue:** a virtual queue $K_b(t) = s(t) - \theta$ that accumulates the charging and discharging amounts, where θ is a perturbation parameter designed to ensure the constraint of the energy state in (10) is satisfied. The dynamic of $K_b(t)$ is given by

$$K_b(t) = K_b(t-1) + \sum_{i \in \mathcal{J}} b_i(t-1). \quad (20)$$

The intuition behind the battery queue $K_b(t)$ is to construct the decision making algorithm based on a quadratic Lyapunov function, then by keeping the quadratic Lyapunov function value small to push the value of $s(t)$ towards θ . Thus, it can be ensured that the battery queue always has enough energy by carefully choosing the value of θ . Note that $K_b(t)$ is a shifted version of the energy state $s(t)$ by a constant parameter θ and can be negative. We will show in Section 4.3 the boundedness of $s(t)$ can be guaranteed through the design of the perturbation parameter θ and V_{max} in (27) and (28).

- **QoS-Aware Load Queue:** a virtual queue $H_{li}(t)$ that is associated with the long-term constraint in (4). It evolves as follows:

$$H_{li}(t+1) = \max \{ H_{li}(t) - \beta_i, 0 \} + \frac{\bar{D}_i(t) - D_i(t)}{\bar{D}_i(t) - \underline{D}_i(t)}. \quad (21)$$

Initialize $H_{li}(t)$ as $H_{li}(0) = 0$. The QoS-aware load queue $H_{li}(t)$ accumulates the portion of unsatisfied flexible load. With the arrival rate being the shedding ratio and the departure rate being β_i in time slot t , the time averaged load shedding ratio must be less than or equal to β_i to ensure the queue $H_{li}(t)$ to be stable. Hence, maintaining the stability of $H_{li}(t)$ is equivalent to keeping the constraint (4) satisfied [21].

By introducing the virtual queues, the time-averaged constraints (4) and (16) are transformed into the mean rate stability constraints of the virtual queues. In the queuing theory, a queue $Q(t)$ is mean rate stable if $\lim_{T \rightarrow \infty} \frac{\mathbb{E}\{Q(t)\}}{T} = 0$, which means the queue does not grow faster than linearly with time. Hence, an optimization problem which minimizes the cost $C_{ToT}(t)$ over time while ensuring that the mean rates of the two virtual queues are kept stable is feasible to **P2**.

We now relax **P2** to **P3**, which is suitable for the Lyapunov optimization framework, as follows:

$$\begin{aligned} \mathbf{P3} : \quad & \min_{\mathbf{Y}(t)} \quad \lim_{T \rightarrow \infty} \frac{1}{T} \sum_{t=0}^{T-1} \mathbb{E} \{ C_{ToT}(t) \}, \\ & \text{s.t.} \quad (2)(5)(6)(7)(9)(20)(21). \end{aligned} \quad (22)$$

Note that, in **P3**, the time-coupled constraint (10) and time-averaged inequality constraint (4) are replaced by mean rate stability constraints (20) and (21), respectively.

4.2. Lyapunov-based Real-time Sharing Control Algorithm Design

In this section, we apply the Lyapunov optimization techniques to solve **P3**. Define $\Theta(t) \triangleq [K_b(t), H_{li}(t)] \forall i \in \mathcal{J}$ as the concatenated vector of the virtual queues. Then a perturbed Lyapunov function is defined as follows:

$$L(\Theta(t)) \triangleq \frac{1}{2} \left[K_b(t)^2 + \sum_{i \in \mathcal{J}} H_{li}(t)^2 \right]. \quad (23)$$

The Lyapunov function $L(\Theta(t))$ is a scalar measure of queue stabilization. Intuitively, if $L(\Theta(t))$ is small then all queues are small; and if $L(\Theta(t))$ is large then at least one queue is large. Thus, by minimizing a drift in the Lyapunov function, i.e., by minimizing a dif-

ference in the Lyapunov function from one slot to the next, queues $K_b(t)$ and $H_{i,i}(t)$ can be stabilized. The conditional one-slot Lyapunov drift, which represents the expected change in the Lyapunov function from one time slot to the next, is defined as follows:

$$\Delta(t) \triangleq \mathbb{E}\{L(t+1) - L(t) | \Theta(t)\}, \quad (24)$$

where the expectation is taken over the random processes associated with the system, given the current queue states $K_b(t)$ and $H_{i,i}(t)$.

We now use the drift-plus-penalty minimization method introduced in the theory of Lyapunov optimization [21] to solve **P3**. In this method, the time-averaged constraints and the objective function are jointly considered. Adding the function of the expected cost in the current time slot, i.e., the penalty function, to (24), we obtain the drift-plus-penalty term $\Delta(t) + V\mathbb{E}\{C_{TOT}(t)\}$, where V , a positive parameter, serves as a weight controlling the performance tradeoff between cost and queueing delay, i.e., how much one cares about the cost compared with the queueing delay. Instead of minimizing the energy consumption cost objective in **P3**, in the Lyapunov optimization, the objective is to minimize the short term drift-plus-penalty function by controlling $\mathbf{Y}(t)$ in each time slot t .

Note that **P3** is a problem of minimizing the time-averaged cost of energy consumption while maintaining the stability of the virtual energy queue and load queue. In the drift-plus-penalty minimization method, minimizing the Lyapunov drift term $\Delta(t)$ of the drift-plus-penalty term alone pushes the queue length of the virtual queues to lower values, while the second term of the drift-plus-penalty term can be viewed as a penalty term with the parameter V controlling the trade-off between minimizing the queue length drift and minimizing the cost function. A larger value of V indicates a greater priority to minimizing the cost function at the cost of a greater size of the virtual queue and vice versa. Thus, by varying the parameter V , one can obtain a desired trade-off between the size of the queue backlogs and the cost of energy consumption. In our case, the maximum feasible V results in the minimized time-averaged cost of energy consumption.

Using the drift-plus-penalty minimization method, a control policy that solves problem **P3** is obtained by minimizing the drift-plus-penalty expression $\Delta(t) + V\mathbb{E}\{C_{TOT}(t)\}$. We first examine the drift-plus-penalty term and obtain an upper bound on it in the following proposition.

Proposition 1. *In each time slot t , for all possible decisions and all possible values of $\Delta(t)$, the drift-plus-penalty term is upper bounded as follows:*

$$\begin{aligned} \Delta(t) + V\mathbb{E}\{C_{TOT}(t)\} &\leq B + K_b(t)\mathbb{E}\left\{\sum_{i \in \mathcal{J}} b_i(t) | \Theta(t)\right\} \\ &+ \sum_{i \in \mathcal{J}} H_{i,i}(t)\mathbb{E}\left\{\frac{D_i(t)-D_i(t)}{D_i(t)-D_i(t)} - \beta_i | \Theta(t)\right\} + V\mathbb{E}\left\{\sum_{i \in \mathcal{J}} C_{MG,i}(t) + \sum_{i \in \mathcal{J}} C_{COM,i}(t)\right\}, \end{aligned} \quad (25)$$

where $B \triangleq \frac{1}{2} \max\{R_{dis}^2, R_{ch}^2\} + \frac{1}{2}(1 + \beta_{max}^2)$ and $\beta_{max} \triangleq \max\{\beta_i : \forall i \in \mathcal{J}\}$.

Proof. See Appendix A ■

With the drift-plus-penalty minimization method, the control decisions are chosen to minimize the upper bound on the Lyapunov drift-plus-penalty obtained in (25) instead of minimizing the drift-plus-penalty expression directly. It will be shown in Section 4.3 that greedily minimizing the upper bound on the Lyapunov

drift-plus-penalty obtained in (25) provides a bounded sub-optimal solution to **P3**. Hence, the real-time sharing control algorithm can be described as follows: in each time slot t , given the system state $\mathbf{X}(t)$ and the queue states $\Theta(t)$, the real-time sharing control algorithm determines the control decision $\mathbf{Y}(t)$ by solving the following linear programming problem **P4**:

$$\begin{aligned} \mathbf{P4} : \quad &\min_{\mathbf{Y}(t)} K_b(t) \sum_{i \in \mathcal{J}} b_i(t) + \sum_{i \in \mathcal{J}} H_{i,i}(t) \frac{D_i(t)-D_i(t)}{D_i(t)-D_i(t)} \\ &+ V \sum_{i \in \mathcal{J}} C_{MG,i}(t) + V \sum_{i \in \mathcal{J}} C_{COM,i}(t) \\ \text{s.t.} \quad &(2)(5)(6)(7)(9)(20)(21). \end{aligned} \quad (26)$$

Although no statistical knowledge associated with the system state $\mathbf{X}(t)$ is required, the queue states $\Theta(t)$ carry sufficient statistical information needed to determine the control decision $\mathbf{Y}(t)$. We will show in Section 4.3 that the design of the real-time problem **P4** can lead to some analytical performance guarantee.

4.3. Algorithm performance analysis

In this section, we analyze the performance of the real-time sharing control algorithm **P4** with respect to the original problem **P1**.

In the following proposition, we prove that the boundedness of the energy states (10) in **P1** can be satisfied by appropriately designing the perturbation parameter θ and the control parameter V . Therefore, the control decisions $\mathbf{Y}(t)$ derived from **P4** are a feasible set of **P1**.

Proposition 2. *In each time slot t , set the perturbation parameter θ as*

$$\theta \triangleq S_{min} + \eta_{dis} R_{dis} + V p_{max}, \quad (27)$$

where

$$0 < V \leq \frac{\eta_{ch}(S_{max} - S_{min} - \eta_{ch} R_{ch} - \eta_{dis} R_{dis})}{p_{max} - p_{min}}. \quad (28)$$

Then, under the real-time sharing control algorithm, given that the system state $\mathbf{X}(t)$ is i.i.d over time, we have

- 1) All the control decisions $\mathbf{Y}(t)$ derived from **P4** are feasible to **P1**, i.e.,

$$S_{min} \leq s(t) \leq S_{max}, \quad \forall t. \quad (29)$$

- 2) The gap between the optimal cost of **P1** and the expected time-averaged cost under the proposed algorithm by solving **P4** is within bound B/V , i.e.,

$$C_{P4}^* - C_{P1}^* \leq \frac{B}{V} \quad (30)$$

where C_{P4}^* is the expected time-averaged cost achieved by **P4**, C_{P1}^* is the optimal cost of **P1**, and $B \triangleq \frac{1}{2} \max\{R_{dis}^2, R_{ch}^2\} + \frac{1}{2}(1 + \beta_{max}^2)$.

Proof. See Appendix B ■

While Proposition 2.1 indicates that, under the real-time sharing control algorithm, the feasibility of the solutions is maintained, Proposition 2.2 characterizes the gap between the resulting time-averaged cost and the optimal cost of **P1**, which is in the order of $O(1/V)$. To minimize this gap, the control parameter V should be set as $V_{max} \triangleq \frac{\eta_{ch}(S_{max} - S_{min} - \eta_{ch} R_{ch} - \eta_{dis} R_{dis})}{p_{max} - p_{min}}$. In other words, under the real-time sharing control algorithm, the time-averaged cost is min-

imized when $V = V_{max}$. Since V_{max} increases with S_{max} , which depends on the shared battery capacity, the real-time sharing control algorithm is asymptotically equivalent to **P1** as the shared battery capacity increases.

In summary, the Lyapunov-based real-time sharing control algorithm provides a low-complexity alternative to achieve a similar performance to the original optimization problem **P1**. However, according to the definition of V_{max} , the proposed algorithm performs better for the shared battery with a larger capacity compared to the one with a smaller capacity.

4.4. Distributed Sharing Control Algorithm

In the previous section, we presented a Lyapunov-based real-time sharing control algorithm to coordinate all households' energy consumption and battery utilization. The real-time problem **P4** can be solved in a centralized way, provided that the solar energy generations and load demand preferences of all the households are all known to a central agent, i.e., all households have to report their renewable generations and demand preferences including the preferred power demands and the QoS control factors, to the central agent. However, this leads to privacy concerns, since the households may not be willing to disclose their private information. In this section, we propose a distributed sharing control algorithm, which is more implementable in practice, to solve the real-time energy management problem **P4** in a distributed manner.

Naturally, in each time slot, based on their solar energy generations and loads, the group of households \mathcal{S} can be divided into two groups: energy surplus group A, \mathcal{S}_a , in which $g_{g_{v,i}} \geq D_i \forall i \in \mathcal{S}_a$, and energy deficit group B, \mathcal{S}_b , in which $g_{g_{v,i}} < D_i \forall i \in \mathcal{S}_b$. Hence, the optimization problem **P4** can be split into two sub-problems for group A and B, respectively:

$$\begin{aligned} \mathbf{P4-a} : \quad & \min_{\mathbf{Y}(t)} K_b(t) \sum_{i \in \mathcal{S}_a} b_i(t) + \sum_{i \in \mathcal{S}_a} H_{l,i}(t) \frac{D_i(t) - \underline{D}_i(t)}{D_i(t) - \underline{D}_i(t)} \\ & + V \sum_{i \in \mathcal{S}_a} C_{MG,i}(t) + V \sum_{i \in \mathcal{S}_a} C_{COM,i}(t) \\ \text{s.t.} \quad & (2)(5)(7)(9)(20)(21), \end{aligned} \quad (31)$$

and

$$\begin{aligned} \mathbf{P4-b} : \quad & \min_{\mathbf{Y}(t)} K_b(t) \sum_{i \in \mathcal{S}_b} b_i(t) + \sum_{i \in \mathcal{S}_b} H_{l,i}(t) \frac{D_i(t) - \underline{D}_i(t)}{D_i(t) - \underline{D}_i(t)} \\ & + V \sum_{i \in \mathcal{S}_b} C_{MG,i}(t) + V \sum_{i \in \mathcal{S}_b} C_{COM,i}(t) \\ \text{s.t.} \quad & (2)(6)(7)(9)(20)(21). \end{aligned} \quad (32)$$

It is noticed that the virtual queue state $K_b(t)$, which is determined by the battery charging and discharging amounts in the previous time slot $t - 1$, can be calculated at the central coordinator side. Thus, in time slot t , assuming $K_b(t)$ is known to all households, the optimization problems in **P4-a** and **P4-b** can be split into sub-problems for each household. Specifically, the sub-problem for each household is

P4-a' for $i \in \mathcal{S}_a$:

$$\begin{aligned} \min_{\mathbf{Y}_i(t)} \quad & K_b(t) b_i(t) + H_{l,i}(t) \frac{\overline{D}_i(t) - D_i(t)}{\overline{D}_i(t) - \underline{D}_i(t)} + VC_i(t) \\ \text{s.t.} \quad & (2)(5)(7)(21), \\ & 0 \leq g_{ch,i}(t) + g_{s,i}(t) \leq \zeta_{ch,i}(t) R_{ch}, \\ & 0 \leq g_{dis,i}(t) \leq \zeta_{dis,i}(t) R_{dis}, \end{aligned} \quad (33)$$

and

P4-b' for $i \in \mathcal{S}_b$:

$$\begin{aligned} \min_{\mathbf{Y}_i(t)} \quad & K_b(t) b_i(t) + H_{l,i}(t) \frac{\overline{D}_i(t) - D_i(t)}{\overline{D}_i(t) - \underline{D}_i(t)} + VC_i(t) \\ \text{s.t.} \quad & (2)(6)(7)(21), \\ & 0 \leq g_{ch,i}(t) + g_{s,i}(t) \leq \zeta_{ch,i}(t) R_{ch}, \\ & 0 \leq g_{dis,i}(t) \leq \zeta_{dis,i}(t) R_{dis}, \end{aligned} \quad (34)$$

where $C_i(t) = C_{MG,i}(t) + C_{COM,i}(t)$, $\zeta_{ch,i}(t)$ and $\zeta_{dis,i}(t)$ represent the percentages of the maximum charging rate and discharging rate, R_{ch} and R_{dis} , taken by household i , respectively. Apparently, in each time slot, as long as $\sum_{i \in \mathcal{S}} \zeta_{ch,i}(t) \leq 1$ and $\sum_{i \in \mathcal{S}} \zeta_{dis,i}(t) \leq 1$, the constraint (9) is satisfied and the solutions to the sub-problems of individual households, **P4-a'** and **P4-b'**, are feasible to **P4**.

We now present a division scheme to divide R_{ch} and R_{dis} among households who request to charge or discharge in a way that allows for not only the requests of households but also their energy contributions to the shared battery. At the beginning of each time slot t , each household first presumes that R_{ch}/R_{dis} is all taken by itself, i.e., $\zeta_{ch,i}(t) = 1$ and $\zeta_{dis,i}(t) = 1 \forall i \in \mathcal{S}$. Based on this presumption in addition to its solar energy generation $g_{pv,i}(t)$ and load demand $\mathbf{d}_i(t)$, each household with energy surplus/deficit calculates its optimal control vector, i.e., the optimal load $D_i(t)$, optimal energy purchasing request for load serving $g_{l,i}(t)$, optimal energy purchasing request for battery charging $g_{s,i}(t)$, optimal battery charging/discharging requests $g_{ch,i}(t)/g_{dis,i}(t)$ by solving the real-time problem **P4-a'**/**P4-b'**.

For the energy surplus group, if the sum of charging requests obtained exceeds the maximum charging rate, the central coordinator proportionally divides the maximum charging rate among households based on the amount of their charging requests, i.e.,

$$\zeta_{ch,i}(t) = \frac{g_{ch,i}(t)}{\sum_{i \in \mathcal{S}_a} g_{ch,i}(t)}.$$

For the energy deficit group, if the sum of discharging requests obtained exceeds the maximum discharging rate, the central coordinator divides the maximum discharging rate among households based on their energy contributions (the accumulated amount of energy it charged and discharged previously), i.e.,

$$\zeta_{dis,i}(t) = \frac{Con_i(t)}{\sum_{i \in \mathcal{S}_b} Con_i(t)},$$

where $Con_i(t)$ is the energy contribution of household i in time slot t , which is given by $Con_i(t) = \sum_{\tau=t-1}^{t-1} \eta_{ch}(g_{ch,i}(\tau) + g_{s,i}(\tau)) - \eta_{dis} g_{dis,i}(\tau)$. Once household i discharges more than its contribution, i.e., $Con_i(t) < 0$, it is only allowed to charge until it has a positive contribution to make sure it restores the discharging amount that exceeds its energy contribution. The central coordinator records the energy contribution of each household. Accordingly, each household redetermines its optimal control vector based on the adjusted value of $\zeta_{ch,i}(t)/\zeta_{dis,i}(t)$.

The real-time distributed sharing control algorithm is summarized in Algorithm 1. With all information obtained locally or through simple communication, under the real-time distributed sharing control algorithm, the optimization problem is solved locally without requiring any statistical information of the system. Thus, the real-time distributed control algorithm not only avoids disclosure of private information but also can be implemented more easily.

Algorithm 1. Real-time Distributed Sharing Control Algorithm

Initialize the virtual battery queue $K_b(0) = s(0) - \theta$, the control parameter $V = V_{max}$, the QoS-aware load queue of each household $H_{l,i}(0) = 0, \forall i$, and the energy contribution of each household $Con_i(1) = 1/I, \forall i$, respectively.

In each time slot, each household executes the following steps sequentially:

1. Receive $K_b(t)$;
2. Initialize $k = 1$ and assume $\xi_{ch,i}^k(t) = 1$ and $\xi_{dis,i}^k(t) = 1$, respectively;
3. Based on its current renewable generation $g_{pv,i}(t)$, demand preferences $d_i(t)$ and virtual QoS-aware load queue $H_{l,i}(t)$, as well as the virtual battery queue state $K_b(t)$, energy price $p(t)$ and upper bounds of charging and discharging rates $\xi_{ch,i}^k(t)R_{ch}$ and $\xi_{dis,i}^k(t)R_{dis}$, solve the real-time problem **P4-a'/P4-b'** to determine its optimal load $D_i^k(t)$, optimal energy purchasing request for load serving $g_{l,i}^k(t)$, optimal energy purchasing request for battery charging $g_{ch,i}^k(t)$, optimal battery charging $g_{ch,i}^k(t)$ and discharging requests $g_{dis,i}^k(t)$;
4. Send its battery charging and discharging requests, $\sum g_{ch,i}^k(t) + g_{s,i}^k(t)$ and $g_{dis,i}^k(t)$, to the central coordinator;
5. $D_i^*(t) \leftarrow D_i^k(t), g_{l,i}^*(t) \leftarrow g_{l,i}^k(t), g_{s,i}^*(t) \leftarrow g_{s,i}^k(t), g_{ch,i}^*(t) \leftarrow g_{ch,i}^k(t)$ and $g_{dis,i}^*(t) \leftarrow g_{dis,i}^k(t)$;
6. Update $H_{l,i}(t)$ based on its evolution equation (21).

In each time slot, the central coordinator executes the following steps sequentially:

1. Initialize $k = 1$, broadcast the control parameter $V = V_{max}$, and virtual battery queue state $K_b(t)$;
 2. After receiving the charging and discharging requests, $\sum g_{ch,i}^k(t) + g_{s,i}^k(t)$ and $g_{dis,i}^k(t)$, from the households, evaluate $\sum_{i \in \mathcal{I}_a} g_{ch,i}^k(t) + g_{s,i}^k(t)$ and $\sum_{i \in \mathcal{I}_b} g_{dis,i}^k(t)$, respectively.
- if** $\sum_{i \in \mathcal{I}_a} g_{ch,i}^k(t) + g_{s,i}^k(t) \leq R_{ch}$ and $\sum_{i \in \mathcal{I}_b} g_{dis,i}^k(t) \leq R_{dis}$ **then**
- a. Inform all households to go to their Step 5;
 - b. $\sum_{i \in \mathcal{I}_a} g_{ch,i}^*(t) + g_{s,i}^*(t) \leftarrow \sum_{i \in \mathcal{I}_a} g_{ch,i}^k(t) + g_{s,i}^k(t)$ and $\sum_{i \in \mathcal{I}_b} g_{dis,i}^*(t) \leftarrow \sum_{i \in \mathcal{I}_b} g_{dis,i}^k(t)$;
 - c. Go to Step 3;
- else**
- a. $k \leftarrow k + 1$;
 - b. $\xi_{ch,i}^k(t) \leftarrow \frac{g_{ch,i}^{k-1}(t) + g_{s,i}^{k-1}(t)}{\sum_{i \in \mathcal{I}_a} g_{ch,i}^{k-1}(t) + g_{s,i}^{k-1}(t)} \forall i \in \mathcal{I}_a$ and $\xi_{dis,i}^k(t) \leftarrow \frac{Con_i(t)}{\sum_{i \in \mathcal{I}_b} Con_i(t)} \forall i \in \mathcal{I}_b$ (if $Con_i(t) < 0$, $\xi_{dis,i}^k(t) = 0$);
 - c. Send $\xi_{ch,i}^k(t)$ and $\xi_{dis,i}^k(t)$ to the respective households and inform all households to repeat their Step 3 and 4;
- end**
3. Update $K_b(t)$ based on its evolution equation (20) and $Con_i(t) \forall i$.

5. Performance evaluation

A performance evaluation of the proposed real-time sharing control algorithm via numerical simulations is provided in this section.

5.1. Simulation setup

We consider a microgrid with I households in the same neighborhood sharing one battery with capacity of S_{cap} , charging and discharging efficiencies of $\eta_{ch} = 0.8$ and $\eta_{dis} = 1.25$, respectively. For the sake of simplicity, we assume that $S_{max} = S_{cap}$ and $S_{min} = 0.1S_{max}$, respectively. In addition, the maximum charging and discharging rates are assumed to be of the same quantity, $R_{ch} = R_{dis} = 0.15S_{max}$. The initial battery energy level is set as S_{min} .

Due to various living habits and some social factors such as the age and type of residence, the load demand of each household in the considered microgrid varies. We simply classify the households into three types: Type I low power consumption, Type II medium power consumption and Type III high power consumption. Each household has a solar PV system with different capacity that generates a different amount of renewable energy everyday from 6 am to 7 pm. We assume households in each type have solar PV systems generating a similar amount of renewable energy everyday, which is selected from a uniform distribution with the mean value of 5 kWh, 8 kWh and 15 kWh and a slight variance of 0.05 kWh for Type I, Type II and Type III, respectively. As shown in the illustrative example in Fig. 2(a), the renewable energy of each household in each time slot is generated using a beta distribution with the mean value of 0.6 kW and the standard deviation of 0.03 kW.

The simulations are run over households with different appliance demand profiles of different types of households. An appliance demand profile generator is developed to simulate the time-varying energy consumption of household appliances for each household in each time slot as shown in Fig. 2(b). With this appliance demand profile generator, each appliance operates in a random time slot during a certain period per day and consumes a certain amount of power selected from a uniform distribution with a different mean for each household type to differentiate power consumption among different types of households, and a variance of 0.2–1 kWh to differentiate power consumption among households in the same type. Note that the main objective of the appliance demand profile generator and the solar energy generation simulator is to simulate the differentiation in load demands and solar energy generations of different households in each time slot to randomly construct the scenario, where some households have surplus solar energy to compete for the free storage space of the battery while others with energy deficit compete for the energy stored in the battery.

The total load demand generated by the appliance demand profile generator for each household in each time slot is used as its maximum energy request $\bar{D}_i(t)$, while the minimum energy demands $\underline{D}_i(t)$ that can not be shed is set randomly from

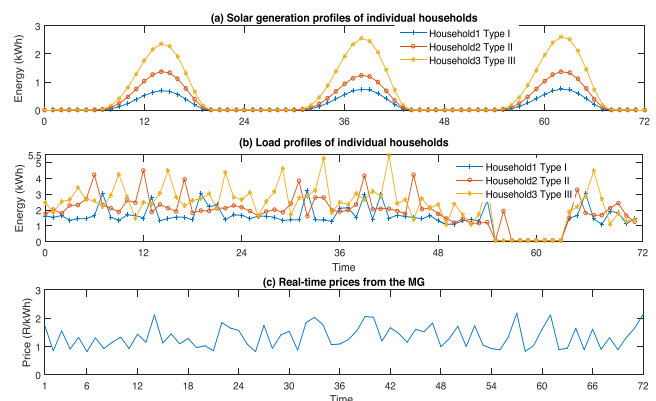


Fig. 2. An example of solar generation profiles and load profiles of individual households as well as real-time prices from the main grid.

Table 1
Comparison of costs and solar generation curtailment rates of the whole microgrid and individual households.

| System Average | H1 | H2 | H3 | H4 | H5 | H6 | H7 | H8 | H9 | H10 | |
|--|---------|---------|---------|---------|---------|---------|---------|---------|---------|---------|---------|
| Household Profile | | | | | | | | | | | |
| Average Monthly Load Demand (kWh) | 1072.14 | 1062.03 | 1304.61 | 880.353 | 1305.55 | 1312.58 | 878.48 | 882.93 | 1302.85 | 1070.14 | |
| Average Monthly Solar Generation (kWh) | 247.50 | 246.67 | 486.18 | 142.36 | 486.82 | 485.13 | 142.39 | 142.37 | 489.22 | 247.01 | |
| Battery Capacity in Distributed ESSs (kWh) | 19.37 | 19.18 | 23.57 | 15.90 | 23.58 | 23.71 | 15.87 | 15.95 | 23.53 | 19.33 | |
| Average Monthly Cost (R) | | | | | | | | | | | |
| Without ESS and DM | 1478.39 | 1456.24 | 1445.45 | 1682.92 | 1233.19 | 1681.39 | 1693.78 | 1228.90 | 1234.11 | 1672.51 | 1455.39 |
| Distributed Sharing Alg | 1067.79 | 1053.63 | 1056.13 | 1161.26 | 944.34 | 1172.38 | 1168.13 | 946.70 | 953.61 | 1161.19 | 1060.48 |
| Greedy Alg 1 TP = 1R/kWh | 1352.27 | 1349.25 | 1340.88 | 1498.77 | 1164.83 | 1497.89 | 1502.28 | 1160.34 | 1166.56 | 1490.10 | 1351.76 |
| Greedy Alg 2 TP = 0.8R/kWh | 1389.38 | 1386.95 | 1377.71 | 1551.32 | 1180.77 | 1551.22 | 1559.95 | 1174.11 | 1183.76 | 1540.49 | 1387.50 |
| Greedy Alg 3 TP = 1.2R/kWh | 1385.75 | 1392.72 | 1382.64 | 1510.44 | 1215.78 | 1513.28 | 1517.21 | 1211.17 | 1217.48 | 1505.74 | 1391.04 |
| Distributed ESSs | 1154.73 | 1154.46 | 1155.27 | 1239.62 | 1033.95 | 1235.85 | 1262.53 | 1035.19 | 1037.35 | 1234.6 | 1158.45 |
| Average Cost per kWh (R/kWh) | | | | | | | | | | | |
| Without ESS and DM | 1.3353 | 1.3583 | 1.3610 | 1.2900 | 1.4008 | 1.2879 | 1.2904 | 1.3989 | 1.3977 | 1.2837 | 1.3600 |
| Distributed Sharing Alg | 1.0757 | 1.0982 | 1.1151 | 0.9843 | 1.2166 | 0.9914 | 0.9817 | 1.2230 | 1.2224 | 0.9839 | 1.1077 |
| Greedy Alg 1 TP = 1R/kWh | 1.2220 | 1.2591 | 1.2632 | 1.1494 | 1.3238 | 1.1479 | 1.1451 | 1.3215 | 1.3219 | 1.1443 | 1.2638 |
| Greedy Alg 2 TP = 0.8R/kWh | 1.2563 | 1.2944 | 1.2980 | 1.1915 | 1.3416 | 1.1898 | 1.1916 | 1.3369 | 1.3411 | 1.1842 | 1.2969 |
| Greedy Alg 3 TP = 1.2R/kWh | 1.2529 | 1.2997 | 1.3025 | 1.1600 | 1.3813 | 1.1607 | 1.1589 | 1.3789 | 1.3791 | 1.1575 | 1.3001 |
| Distributed ESSs | 1.1432 | 1.1563 | 1.1676 | 1.0363 | 1.2498 | 1.0298 | 1.0428 | 1.2505 | 1.2450 | 1.0285 | 1.1612 |
| Solar Generation Curtailment Rate | | | | | | | | | | | |
| Distributed Sharing Alg | 5.35% | 5.29% | 5.28% | 5.39% | 4.97% | 5.42% | 5.47% | 5.03% | 5.03% | 5.51% | 5.34% |
| Greedy Alg 1 TP = 1R/kWh | 25.25% | 24.50% | 24.47% | 25.90% | 23.23% | 26.07% | 25.91% | 23.23% | 23.24% | 26.09% | 24.41% |
| Greedy Alg 2 TP = 0.8R/kWh | 29.26% | 28.35% | 28.28% | 30.04% | 26.67% | 30.27% | 30.12% | 26.66% | 26.66% | 30.39% | 28.25% |
| Greedy Alg 3 TP = 1.2R/kWh | 20.86% | 20.19% | 20.13% | 21.39% | 19.11% | 21.63% | 21.41% | 19.11% | 19.19% | 21.62% | 20.10% |
| Distributed ESSs | 9.03% | 1.16% | 2.72% | 13.36% | 0 | 14.02% | 13.74% | 0 | 0 | 13.44% | 2.49% |

TP stands for threshold price.

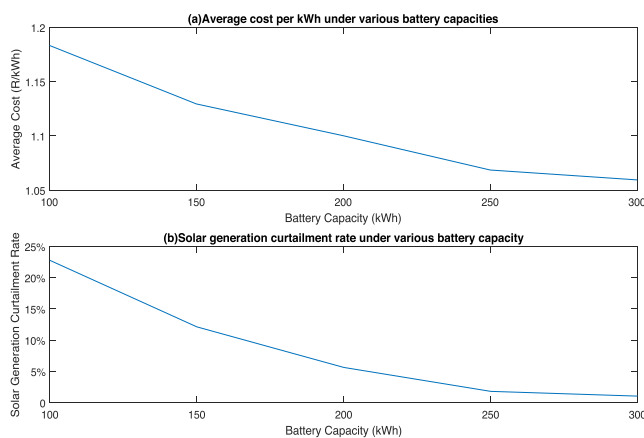


Fig. 3. Average cost per kWh and solar generation curtailment rate under various battery capacities.

$[0.3\bar{D}_i(t), 0.7\bar{D}_i(t)]$. The QoS related parameters $\alpha_i(t)$ for each household in each time slot and β_i for each household are chosen randomly from $[1.5, 3.5]$ and $[0.5, 0.7]$, respectively. In addition,

as shown in Fig. 2(c), the time-varying energy price from the main grid $p(t)$ is uniformly distributed between 0.8 and 2.2R/kWh with the mean of 1.5R/kWh.

5.2. Simulation results

This section presents simulation results of the proposed distributed sharing control algorithm. We consider a period of 90 days, where $T = 2160$ with each time slot representing 1 h, and randomly generate 10 households consisting of 3 Type I households with an average daily load demand of 29.35 kWh, 3 Type II households with an average daily load demand of 35.60 kWh and 4 Type III households with an average daily load demand of 58.06 kWh. In total, the 10 households have a daily average of 427.09 kWh of load demand and a daily average of 103.85 kWh of solar generation. The average monthly load demands and solar generations of individual households are listed in Table 1 for the sake of easy comparison. The real-time optimization problem in P4 is solved using the CVX toolbox [30] for Matlab.

By varying the battery capacity, we investigate the effectiveness of the shared battery in cost saving in this battery sharing system. As can be observed in Fig. 3(b), the solar generation curtailment

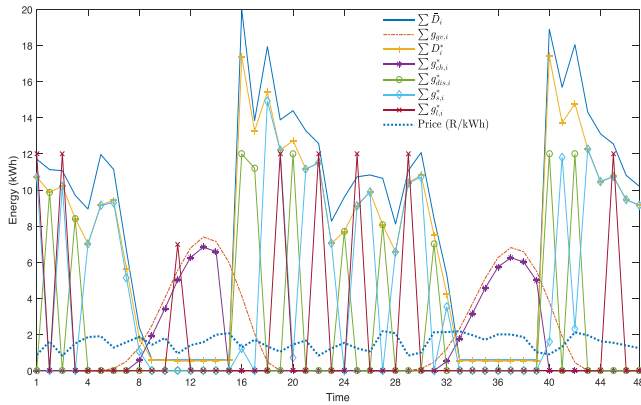


Fig. 4. Real-time system states $X(t)$ and control decisions $Y(t)$ of the proposed distributed sharing control algorithm.

rate drops with an increase in the battery capacity since there is more storage capacity to accommodate surplus solar generations and cheaper electricity from the MG. Accordingly, the average cost per kWh decreases with the increase in the battery capacity as shown in Fig. 3(a). Obviously, considering the relatively high initial investment cost of batteries, which is expressed on a per kWh of energy capacity basis, a trade-off between battery capacity, solar generation curtailment, electricity consumption cost along with other factors should be made in sizing the shared battery, so that the battery sharing system achieves optimal cost-benefit ratio. However, in this work, we mainly concentrate on how to utilize the shared storage given the dynamic behavior of the system to reduce electricity consumption cost and do not consider the optimal sizing of the shared battery. In the following, we further investigate the performance of the proposed sharing control algorithm using a battery sharing system with the 10 households sharing a 200 kWh battery, which is enough to accommodate the load demands with a relatively low cost and near zero solar generation curtailment (shown in Fig. 3), as an example. The average monthly load demands and corresponding average monthly cost without a battery storage and a demand management mechanism are listed Table 1 as lower bounds.

In order to evaluate the performance of the proposed distributed sharing control algorithm, a greedy sharing algorithm, where each household is myopic and only aims to minimize its current cost without taking the future and other households into account, is used for comparison. Specifically, under this myopic greedy sharing algorithm, assuming that all storage space and energy available in the shared battery can be used by itself, each household independently solves a simple cost minimization problem in (35) to derive its optimal charging (energy generated by its solar energy generation and purchased from the MG) and discharging requests as well as the optimal energy consumption of its controllable loads. To ensure that the space-availability constraint and the energy-availability constraint in (11) are satisfied, if the sum of the amounts of charge and/or discharge from all households exceeds the storage space and/or energy available in the shared battery, the storage space and/or energy available for charging/discharging is proportionally divided among the households based on the amounts of their charging requests and/or their energy contributions.

$$\begin{aligned} \min_{Y(t)} & [g_{l,i}(t) + g_{s,i}(t)]p(t) + \alpha_i(t) [D_i^-(t) - D_i(t)]^2, \quad \forall i \in \mathcal{I}, \\ \text{s.t.} & (2)(5)(6)(7)(8)(11) \quad \frac{D_i(t) - D_i(t)}{D_i(t) - D_i(t)} \leq \beta_i, \quad \forall i \in \mathcal{I}. \end{aligned} \tag{35}$$

Note that, since there is no load management mechanism in the greedy algorithm, the constraint $\frac{D_i(t) - D_i(t)}{D_i(t) - D_i(t)} \leq \beta_i$ is added to make sure that the QoS of each household is satisfied. Moreover, to allow the greedy sharing algorithm to take advantage of the time-varying pricing, if there is storage space for charging, each household purchases energy from the MG as long as the price is lower than a certain price, which is called threshold price. Note that, under the greedy sharing algorithm, since purchasing energy to charge into the battery mostly depends on the threshold price, there could be unnecessary energy purchases, which in turn leads to increases in the average cost per kWh and solar generation curtailment. In the comparison, the threshold price is first set as 1R/kWh. The threshold price will be varied later on to provide a more complete comparison.

It can be observed that, in Fig. 5, under the greedy sharing algorithm, as long as there is storage space, energy is purchased to charge into the battery when the price is lower than the threshold price, which results in a situation where there is less storage space for the generated solar energy. In contrast, as shown in Fig. 4, with the systematic optimization mechanism in the proposed sharing control algorithm, energy is purchased to charge into the shared battery with lower prices when necessary, and the solar energy generation takes precedence when making charging decision. As can be observed in Fig. 6, which compares the real-time prices from the MG and the real-time costs of individual households incurred under the proposed sharing control algorithm, the spikes of the real-time costs of each household coincide with the drops in the prices. It can be explained as follows: with the Lyapunov optimization based sharing control algorithm, purchasing energy to charge to the shared battery if necessary only occurs when the price from the MG is lower. In general, as shown in Fig. 7, the SoC of the shared battery under the greedy sharing algorithm (with the average SoC level being 38.41 kW).

Fig. 8 provides a comparison of the accumulated served load and corresponding cost over time. The accumulated original demand and corresponding cost (with an average monthly cost of R1478.39 as listed in Table 1) without a battery storage and a demand management mechanism are shown as lower bounds. It is illustrated that the proposed sharing control algorithm with an average monthly cost of R1067.79 outperforms the myopic greedy algorithm with an average monthly cost of R1351.75. In addition, as shown in both Figs. 5 and 8, without a proper load management mechanism, the greedy sharing algorithm has to serve more energy consumption (with the average shed demand rate being 0.05%) with a higher average cost per kWh (1.22R/kWh) compared to that of the proposed algorithm (1.08R/kWh) with an average shed demand rate of 10.34%, as listed in Table 1. Table 1 also shows that,

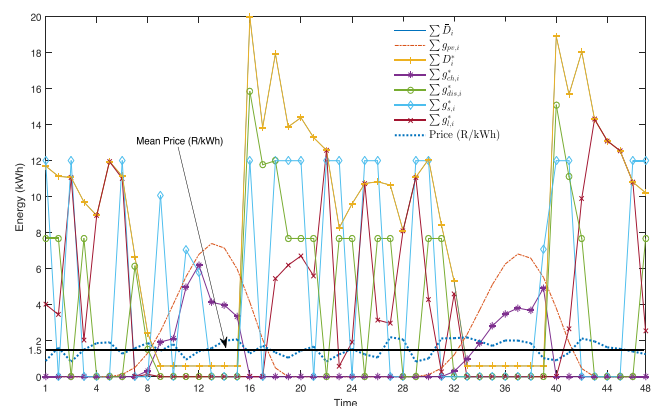


Fig. 5. Real-time inputs and outputs of the greedy sharing algorithm.

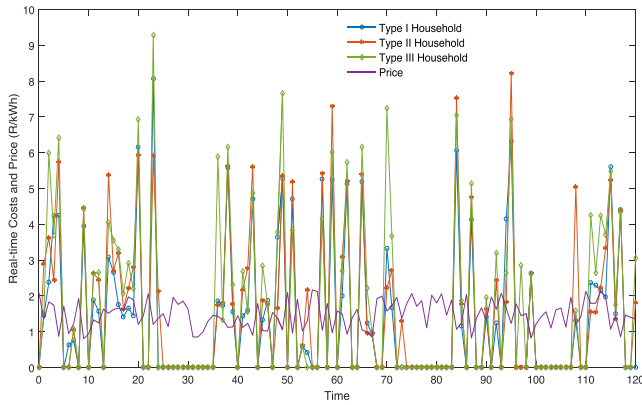


Fig. 6. Real-time prices from the main grid and real-time costs.

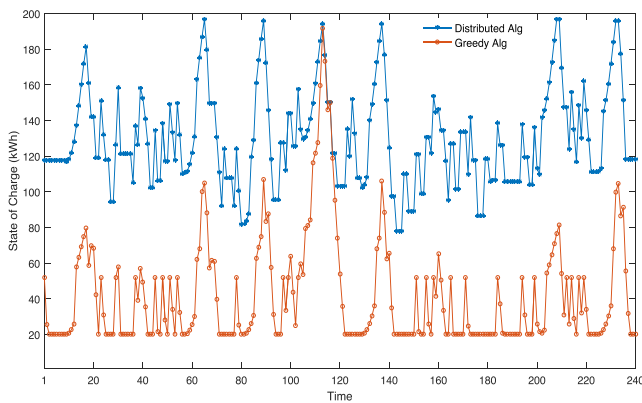


Fig. 7. State of Charge.

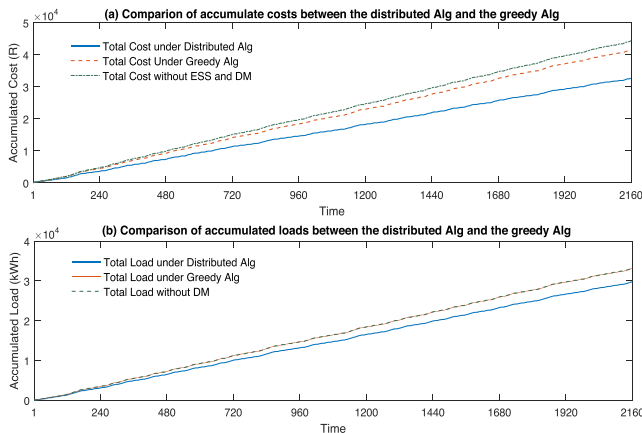


Fig. 8. Comparison of accumulated costs and loads between the proposed algorithm and the greedy algorithm.

compared to the greedy algorithm, the proposed sharing control algorithm reduces the average monthly cost and solar generation curtailment of each individual household by 19.11%–22.25% and 79.20%–79.21%, respectively.

As mentioned above, under the greedy sharing algorithm, the choice of the threshold price has an impact on the average cost per kWh and solar generation curtailment. To show the influence of the threshold price, the total 30-day costs, the average costs per kWh and the solar generation curtailment rates under the greedy sharing algorithm with varying threshold prices are com-

pared in Table 1. Note that, when the threshold price is set as the lowest price 0.8R/kWh, there is no purchased energy to charge into the shared battery. It is shown that, the greedy sharing algorithm with the threshold price being 1R/kWh achieves the lowest costs but wastes more solar generation compared to the case with the threshold price being 1.2R/kWh, as the energy purchased to charge into the battery leads to less storage space for the generated solar energy. In general, under the greedy sharing algorithm, less generated solar energy can be accommodated. Thus, the proposed sharing control algorithm significantly reduces the energy costs of individual households while avoiding solar generation curtailment more effectively.

In addition, to investigate the effectiveness of the proposed sharing algorithm that is able to take advantage of the non-overlapping power consumption patterns of users, the proposed distributed sharing system is compared with a distributed ESSs case, where each household individually owns an ESS. The battery capacity of individual household is set in proportion to its net load demand (the load demand minus the renewable generation that can be used to serve the load directly) while the overall capacity of all households is equivalent to the capacity of the shared battery in the sharing system. Specifically, the battery capacity of household i is equal to $\rho_i E_{max}$, where $\rho_i = \frac{\sum_{t=0}^{T-1} \bar{D}_i(t) - g_{pv,i}(t)}{\sum_{i=1}^J \sum_{t=0}^{T-1} \bar{D}_i(t) - g_{pv,i}(t)}$ and E_{max} is the capacity of the shared battery in the sharing system. For a fair comparison, in the distributed ESSs case, each household operates its ESS with a similar control scheme using the Lyapunov optimization technique. As shown in Table 1, compared to the distributed ESSs case, households with a shared battery achieve 5.14%–8.73% lower average monthly costs while reducing 40.75% solar generation curtailment in total. This indicates that, by coordinating the utilization of the shared battery among households, the solar generation curtailment can be avoided more effectively, which in turn leads to energy cost reduction.

6. Conclusions

In this work, a smart community that is comprised of a group of households with renewable energy sources and controllable loads sharing a common battery is considered. An ESSM system, in which households cooperatively utilize the shared battery, is presented, aiming to minimize the long term time-averaged cost of the whole system, i.e., the long-term time-averaged costs of all households, subject to the operational constraints of the shared battery as well as the arbitrary dynamics of renewable generations, load demands, and electricity pricing. We study the energy management problem for such an energy storage sharing system and propose a distributed real-time sharing control algorithm based on the Lyapunov theory to coordinate households to optimally utilize the shared battery by jointly optimizing charging and discharging of the shared ESS as well as the energy consumption of all households in a distributed manner without requiring any system statistics. The proposed distributed sharing control algorithm is easy to implement practically while preserving privacy. It is shown that, the proposed sharing control algorithm leverages the price variations while taking the surplus PV generations into consideration to reduce the electricity consumption costs by selecting proper time slots to purchase cheaper electricity from the MG if necessary. Compared to the greedy sharing algorithm and the distributed ESSs case, the proposed sharing control algorithm can save power consumption cost while improving the utilization of renewable energy generation.

There are several possible directions to extend the work in the future. First, a compelling extension of the proposed sharing scheme would be the incorporation of battery degradation and life-

cycle effects into the battery storage management. Secondly, as forecasts of the system states (e.g., solar generations and loads) can be available within a certain time interval, it would be interesting to study how to incorporate these forecasts into the battery sharing management system.

CRedit authorship contribution statement

Khmaies Ouahada: Conceptualization, Methodology, Supervision, Writing - review & editing. **Hailing Zhu:** Conceptualization, Formal analysis, Investigation, Methodology, Validation, Writing-original draft & editing.

Declaration of Competing Interest

The authors declare that they have no known competing financial interests or personal relationships that could have appeared to influence the work reported in this paper.

Appendix A. Proof of Proposition 1

According to the definition of $L(\Theta(t))$, the difference

$$L(\Theta(t+1)) - L(\Theta(t)) = \frac{1}{2} [K_b(t+1)^2 - K_b(t)^2] + \sum_{i \in \mathcal{J}} \frac{1}{2} [H_{li}(t+1)^2 - H_{li}(t)^2] \tag{36}$$

Based on the queue update of $K_b(t)$ in (20), the term $K_b(t+1)^2 - K_b(t)^2$ in (36) can be upper bounded by

$$K_b(t+1)^2 - K_b(t)^2 \leq 2K_b(t) \sum_{i \in \mathcal{J}} b_i(t) + \max\{R_{dis}^2, R_{ch}^2\}. \tag{37}$$

Similarly, based on the queue update of $H_{li}(t)$ in (21), the term $H_{li}(t+1)^2 - H_{li}(t)^2$ in (36) can be upper bounded by

$$H_{li}(t+1)^2 - H_{li}(t)^2 \leq 2H_{li}(t) \left[\frac{\bar{D}_i(t) - D_i(t)}{\bar{D}_i(t) - \underline{D}_i(t)} - \beta_i \right] + 1 + \beta_i^2. \tag{38}$$

Applying inequalities (37) and (38) to (36), taking the conditional expectation over $L(\Theta(t+1)) - L(\Theta(t))$ given $\Theta(t)$ and adding the term $V\mathbb{E}\{C_{TOT}(t)\}$ yield the upper bound in (25).

Appendix B. Proof of Proposition 2

Proof of Proposition 2:

The per-slot problem **P4** includes all constraints of the original problem **P1** except for the energy state constraint. Hence, to prove the solution derived from **P4** are feasible to **P1** is to show the energy state $s(t)$ is bounded within $[S_{min}, S_{max}]$. The optimization problem **P4** can be rearranged to **P5**

$$\begin{aligned} \mathbf{P5} : \quad & \min_{\mathbf{Y}(t)} [Vp(t) + K_b(t)\eta_{ch}] \sum_{i \in \mathcal{J}} g_{s,i}(t) + K_b(t)\eta_{ch} \sum_{i \in \mathcal{J}} g_{ch,i}(t) \\ & + Vp(t) \sum_{i \in \mathcal{J}} g_{li}(t) - K_b(t)\eta_{dis} \sum_{i \in \mathcal{J}} g_{dis,i}(t) \\ & + V \sum_{i \in \mathcal{J}} \alpha_i [\bar{D}_i(t) - D_i(t)]^2 + \sum_{i \in \mathcal{J}} H_{li}(t) \frac{\bar{D}_i(t) - D_i(t)}{\bar{D}_i(t) - \underline{D}_i(t)}, \end{aligned} \tag{39}$$

s.t. (5)(6)(7)(2)(9)(20)(21).

Let $\mathbf{D}^*(t) \triangleq [D_i^*(t)]$, $\mathbf{g}_{ch}^*(t) \triangleq [g_{ch,i}^*(t)]$, $\mathbf{g}_{dis}^*(t) \triangleq [g_{dis,i}^*(t)]$, $\mathbf{g}_i^*(t) \triangleq [g_{li}^*(t)]$ and $\mathbf{g}_s^*(t) \triangleq [g_{s,i}^*(t)] \forall i \in \mathcal{J}$ be the optimal solution to (39). It is noticed that $\mathbf{D}^*(t)$ will not directly affect the battery queue $K_b(t)$. Hence, $\mathbf{D}^*(t)$ can be treated as a given load. As mentioned previously, we consider two cases in determining how to utilize the solar energy generation: **Case 1:** energy surplus where $g_{gv,i}(t) \geq D_i^*(t)$

and **Case 2:** energy deficit where $g_{gv,i}(t) < D_i^*(t)$. Thus, the user group I can be naturally divided into two groups: group A, \mathcal{J}_a , where $g_{gv,i}(t) \geq D_i^*(t) \forall i \in \mathcal{J}_a$, and group B, \mathcal{J}_b , where $g_{gv,i}(t) < D_i^*(t) \forall i \in \mathcal{J}_b$. Correspondingly, the optimization problem **P5** can be split into two per-slot sub-problems for group A and B, respectively, as follows:

- **Case 1:** when $g_{gv,i}(t) \geq D_i^*(t)$, we have $g_{li}^*(t) = 0$. Then, the optimization problem for group A **P5-a** is written as:

$$\begin{aligned} \mathbf{P5-a} : \quad & \text{Energy Surplus} \\ \min_{\mathbf{Y}(t)} \quad & [Vp(t) + K_b(t)\eta_{ch}] \sum_{i \in \mathcal{J}_a} g_{s,i}(t) + K_b(t)\eta_{ch} \sum_{i \in \mathcal{J}_a} g_{ch,i}(t) \\ & - K_b(t)\eta_{dis} \sum_{i \in \mathcal{J}_a} g_{dis,i}(t) + V \sum_{i \in \mathcal{J}_a} \alpha_i [\bar{D}_i(t) - D_i(t)]^2 \\ & + \sum_{i \in \mathcal{J}_a} H_{li}(t) \frac{\bar{D}_i(t) - D_i(t)}{\bar{D}_i(t) - \underline{D}_i(t)} \end{aligned}$$

s.t. (2)(9)(20)(21). (40)

- **Case 2:** when $g_{gv,i}(t) < D_i^*(t)$, according to (6), we have $g_{ch,i}^*(t) = 0$ and $g_{li}^*(t) = D_i^*(t) - g_{dis,i}^*(t) - g_{pv,i}(t)$. Then, the optimization problem for group B **P5-b** is written as:

$$\begin{aligned} \mathbf{P5-b} : \quad & \text{Energy Deficit} \\ \min_{\mathbf{Y}(t)} \quad & [Vp(t) + K_b(t)\eta_{ch}] \sum_{i \in \mathcal{J}_b} g_{s,i}(t) - K_b(t)\eta_{dis} \sum_{i \in \mathcal{J}_b} g_{dis,i}(t) \\ & + Vp(t) \sum_{i \in \mathcal{J}_b} [D_i(t) - g_{dis,i}(t) - g_{pv,i}(t)] \\ & + V \sum_{i \in \mathcal{J}_b} \alpha_i [\bar{D}_i(t) - D_i(t)]^2 + \sum_{i \in \mathcal{J}_b} H_{li}(t) \frac{\bar{D}_i(t) - D_i(t)}{\bar{D}_i(t) - \underline{D}_i(t)} \\ = \quad & [Vp(t) + K_b(t)\eta_{ch}] \sum_{i \in \mathcal{J}_b} g_{s,i}(t) - Vp(t) \sum_{i \in \mathcal{J}_b} g_{pv,i}(t) \\ & - [Vp(t) + K_b(t)\eta_{dis}] \sum_{i \in \mathcal{J}_b} g_{dis,i}(t) + Vp(t) \sum_{i \in \mathcal{J}_b} D_i(t) \\ & + V \sum_{i \in \mathcal{J}_b} \alpha_i [\bar{D}_i(t) - D_i(t)]^2 + \sum_{i \in \mathcal{J}_b} H_{li}(t) \frac{\bar{D}_i(t) - D_i(t)}{\bar{D}_i(t) - \underline{D}_i(t)} \end{aligned}$$

s.t. (2)(9)(20)(21). (41)

By combining **P5-a** and **P5-b** together, the optimization problem **P5** is transformed into the following optimization problem:

$$\begin{aligned} \mathbf{P6} : \quad & \min_{\mathbf{Y}(t)} [Vp(t) + K_b(t)\eta_{ch}] \sum_{i \in \mathcal{J}} g_{s,i}(t) + K_b(t)\eta_{ch} \sum_{i \in \mathcal{J}_a} g_{ch,i}(t) \\ & - [Vp(t) + K_b(t)\eta_{dis}] \sum_{i \in \mathcal{J}_b} g_{dis,i}(t) - K_b(t)\eta_{dis} \sum_{i \in \mathcal{J}_a} g_{dis,i}(t) \\ & + Vp(t) \sum_{i \in \mathcal{J}_b} D_i(t) + V \sum_{i \in \mathcal{J}} \alpha_i [\bar{D}_i(t) - D_i(t)]^2 \\ & + \sum_{i \in \mathcal{J}} H_{li}(t) \frac{\bar{D}_i(t) - D_i(t)}{\bar{D}_i(t) - \underline{D}_i(t)} \end{aligned} \tag{42}$$

s.t. (2)(9)(20)(21).

Note that the optimal solution to **P6** has the following properties:

- If $K_b(t) > -Vp_{min}/\eta_{ch}$, $\sum_{i \in \mathcal{J}} g_{s,i}^* = 0$;
- If $K_b(t) < -Vp_{max}/\eta_{ch}$, $\sum_{i \in \mathcal{J}} g_{s,i}^* + g_{ch,i}^* = R_{ch}$.

We now prove the boundary of $s(t)$ in (29) using induction. First it is obvious that the lower and upper bounds hold for $t = 0$. Now suppose that the boundary holds for time slot t , i.e., $S_{min} \leq s(t) \leq S_{max}$. This in turn indicates $S_{min} - \theta \leq K_b(t) \leq S_{max} - \theta$, i.e., $-Vp_{max}/\eta_{ch} - \eta_{dis}R_{dis} \leq K_b(t) \leq S_{max} - S_{min} - Vp_{max}/\eta_{ch} - \eta_{dis}R_{dis}$.

Hence, to prove the boundary of $s(t)$ in (29) also holds for time slot $t + 1$, we need to prove the boundary of $K_b(t)$, i.e., $[-Vp_{max}/\eta_{ch} - \eta_{dis}R_{dis}, S_{max} - S_{min} - Vp_{max}/\eta_{ch} - \eta_{dis}R_{dis}]$, holds for time slot $t + 1$. We consider the following cases:

- 1) First suppose $-Vp_{max}/\eta_{ch} - \eta_{dis}R_{dis} \leq K_b(t) < -Vp_{max}/\eta_{ch}$, we have $\sum_{i \in \mathcal{I}} (g_{s,i}^* + g_{ch,i}^*) = R_{ch}$, $\sum_{i \in \mathcal{I}_a} g_{pv,i}^* = 0$ and $\sum_{i \in \mathcal{I}_a} g_{dis,i}^* = 0$. Then, based on (20), the battery queue $K_b(t)$ updates as follows:

$$K_b(t+1) = K_b(t) + \eta_{ch} \sum_{i \in \mathcal{I}} (g_{s,i}^* + g_{ch,i}^*) - \eta_{dis} \sum_{i \in \mathcal{I}} g_{dis,i}^* \\ = K_b(t) + \eta_{ch} R_{ch} > K_b(t) \geq -Vp_{max}/\eta_{ch} - \eta_{dis}R_{dis}.$$

In addition, as $K_b(t) < -Vp_{max}/\eta_{ch}$, we have

$$K_b(t+1) < -Vp_{max}/\eta_{ch} + \eta_{ch}R_{ch} \leq S_{max} - S_{min} - Vp_{max}/\eta_{ch} - \eta_{dis}R_{dis},$$

as long as $S_{max} - S_{min} - \eta_{dis}R_{dis} - \eta_{ch}R_{ch} \geq 0$ holds.

- 2) Secondly, suppose $-Vp_{min}/\eta_{ch} \leq K_b(t) \leq -Vp_{min}/\eta_{ch}$,
 - a) if $K_b(t) \geq -Vp(t)/\eta_{ch}$, we have $\sum_{i \in \mathcal{I}_a} g_{s,i}^* = 0$. There are two possibilities to study:
 - i) when $-Vp(t)/\eta_{ch} \leq K_b(t) < -Vp(t)/\eta_{dis}$, we have $\sum_{i \in \mathcal{I}_a} g_{ch,i}^* = \min\{R_{ch}, \sum_{i \in \mathcal{I}_a} (g_{pv,i} - D_i^*)\}$ and $\sum_{i \in \mathcal{I}_a} g_{dis,i}^* = 0$. Thus,

$$K_b(t+1) = K_b(t) + \eta_{ch} \min\left\{R_{ch}, \sum_{i \in \mathcal{I}_a} (g_{pv,i} - D_i^*)\right\} \\ > K_b(t) \geq -Vp_{max}/\eta_{ch} - \eta_{dis}R_{dis}.$$

In addition, as $K_b(t) < -Vp_{min}/\eta_{ch}$, we have

$$K_b(t+1) < -Vp_{min}/\eta_{ch} + \eta_{ch}R_{ch} \\ \leq S_{max} - S_{min} - Vp_{max}/\eta_{ch} - \eta_{dis}R_{dis},$$

based on the definition $V \leq \frac{\eta_{ch}(S_{max} - S_{min} - \eta_{ch}R_{ch} - \eta_{dis}R_{dis})}{P_{max} - P_{min}}$ in (28).

- ii) when $-Vp(t)/\eta_{dis} \leq K_b(t) \leq -Vp_{min}/\eta_{ch}$, we have

$\sum_{i \in \mathcal{I}_a} g_{ch,i}^* = \min\{R_{ch}, \sum_{i \in \mathcal{I}_a} (g_{pv,i} - D_i^*)\}$ and $\sum_{i \in \mathcal{I}_a} g_{dis,i}^* = \min\{R_{dis}, \sum_{i \in \mathcal{I}_a} (D_i^* - g_{pv,i})\}$. In other words, the maximum possible increase is $\eta_{ch}R_{ch}$ and the maximum possible decrease is $\eta_{dis}R_{dis}$. Thus, using the upper bound of V as the case above, we have

$$K_b(t+1) < K_b(t) + \eta_{ch}R_{ch} \leq -Vp_{min}/\eta_{ch} + \eta_{ch}R_{ch} \\ \leq S_{max} - S_{min} - Vp_{max}/\eta_{ch} - \eta_{dis}R_{dis},$$

while

$$K_b(t+1) > K_b(t) - \eta_{dis}R_{dis} \geq -Vp_{max}/\eta_{ch} - \eta_{dis}R_{dis}.$$

- b) if $K_b(t) < -Vp(t)/\eta_{ch}$, we have $\sum_{i \in \mathcal{I}_a} g_{s,i}^* + \sum_{i \in \mathcal{I}_a} g_{ch,i}^* = R_{ch}$ and $\sum_{i \in \mathcal{I}_a} g_{dis,i}^* = 0$. Thus, using the upper bound of V as the case above, we have

$$K_b(t+1) = K_b(t) + \eta_{ch}R_{ch} \leq -Vp_{min}/\eta_{ch} + \eta_{ch}R_{ch} \\ \leq S_{max} - S_{min} - Vp_{max}/\eta_{ch} - \eta_{dis}R_{dis},$$

while

$$K_b(t+1) = K_b(t) + \eta_{ch}R_{ch} \geq -Vp_{max}/\eta_{ch} + \eta_{ch}R_{ch} \\ > -Vp_{max}/\eta_{ch} - \eta_{dis}R_{dis},$$

- 3) Thirdly, suppose $-Vp_{min}/\eta_{ch} < K_b(t) \leq 0$, we have $\sum_{i \in \mathcal{I}_a} g_{s,i}^* = 0$. As the case 2.a above, we consider two possibilities as follows:

- a) when $-Vp_{min}/\eta_{ch} < K_b(t) \leq -Vp_{min}/\eta_{dis}$, we have $\sum_{i \in \mathcal{I}_a} g_{ch,i}^* = \min\{R_{ch}, \sum_{i \in \mathcal{I}_a} (g_{pv,i} - D_i^*)\}$ and $\sum_{i \in \mathcal{I}_a} g_{dis,i}^* = 0$. Thus,

$$K_b(t+1) = K_b(t) + \eta_{ch} \min\left\{R_{ch}, \sum_{i \in \mathcal{I}_a} (g_{pv,i} - D_i^*)\right\} \\ > -Vp_{min}/\eta_{ch} > -Vp_{max}/\eta_{ch} - \eta_{dis}R_{dis}.$$

In addition, as $K_b(t) > -Vp_{min}/\eta_{dis}$, we have

$$K_b(t+1) < -Vp_{min}/\eta_{dis} + \eta_{ch}R_{ch} \\ \leq S_{max} - S_{min} - Vp_{max}/\eta_{ch} - \eta_{dis}R_{dis},$$

- b) when $K_b(t) \geq -Vp_{min}/\eta_{dis}$, we have $\sum_{i \in \mathcal{I}_a} g_{ch,i}^* = \min\{R_{ch}, \sum_{i \in \mathcal{I}_a} (g_{pv,i} - D_i^*)\}$ and $\sum_{i \in \mathcal{I}_a} g_{dis,i}^* = \min\{R_{dis}, \sum_{i \in \mathcal{I}_a} (D_i^* - g_{pv,i})\}$. In other words, the maximum possible increase is R_{ch} and the maximum possible decrease is R_{dis} . Thus, using the upper bound of V as the case above, we have

$$K_b(t+1) < K_b(t) + \eta_{ch}R_{ch} \leq -Vp_{min}/\eta_{dis} + \eta_{ch}R_{ch} \\ \leq S_{max} - S_{min} - Vp_{max}/\eta_{ch} - \eta_{dis}R_{dis},$$

while

$$K_b(t+1) > K_b(t) - \eta_{dis}R_{dis} \geq -\eta_{dis}R_{dis} > -Vp_{max}/\eta_{ch} - \eta_{dis}R_{dis}.$$

- 4) Finally, suppose $0 < K_b(t) \leq S_{max} - S_{min} - Vp_{max}/\eta_{ch} - \eta_{dis}R_{dis}$, we have

$$\sum_{i \in \mathcal{I}} g_{s,i}^* = 0, \sum_{i \in \mathcal{I}} g_{ch,i}^* = 0$$

$$\text{and } \sum_{i \in \mathcal{I}} g_{dis,i}^* = \min\left\{R_{dis}, \sum_{i \in \mathcal{I}} (D_i^* - g_{pv,i})\right\}.$$

Hence,

$$K_b(t+1) = K_b(t) - \eta_{dis} \min\left\{R_{dis}, \sum_{i \in \mathcal{I}} (D_i^* - g_{pv,i})\right\} \\ < K_b(t) \leq S_{max} - S_{min} - Vp_{max}/\eta_{ch} - \eta_{dis}R_{dis}.$$

In addition, as $K_b(t) > 0$, we have

$$K_b(t+1) = K_b(t) - \eta_{dis} \min\left\{R_{dis}, \sum_{i \in \mathcal{I}} (D_i^* - g_{pv,i})\right\} \\ > -\eta_{dis} \min\left\{R_{dis}, \sum_{i \in \mathcal{I}} (D_i^* - g_{pv,i})\right\} > -\eta_{dis}R_{dis} > -Vp_{max}/\eta_{ch} - \eta_{dis}R_{dis}.$$

From the induction, the boundary of $s(t)$ in (29) holds for any time slot with any control decisions derived from **P4**, which indicates that all constraints of **P1** are satisfied. Hence, all control decisions derived from **P4** are feasible to **P1**.

Proof of Proposition 2.2:

To prove Proposition 2.2, we first give the following lemma, which can be derived from Theorem 4.5 in [21].

Lemma 1. *There exists a stationary and randomized control policy Π that achieves the following:*

$$\mathbb{E}\{C^\Pi(t)\} = C_{P1}^*; \tag{43}$$

$$\mathbb{E}\left\{\sum_{i \in \mathcal{I}} b_i^\Pi(t)\right\} = 0; \tag{44}$$

$$\mathbb{E}\left\{\frac{\bar{D}_i(t) - D_i^\Pi(t)}{\bar{D}_i(t) - \underline{D}_i(t)}\right\} \leq \beta_i, \tag{45}$$

where all expectations are taken over the randomness of the system state and the possible randomness of the energy charging/discharging and purchasing decisions.

Since the proposed algorithm is to minimize the RHS of (25), the value of the RHS should be smaller than that under the policy Π , which yield:

$$\begin{aligned} \Delta(t) + V\mathbb{E}\{C_{p4}^*(t)\} &\leq B + K_b(t)\mathbb{E}\left\{\sum_{i \in \mathcal{J}} b_i^\Pi(t) |\Theta(t)\right\} \\ + \sum_{i \in \mathcal{J}} H_{i,i}(t)\mathbb{E}\left\{\frac{D_i(t) - D_i^\Pi(t)}{D_i(t) - D_i(t)} - \beta_i |\Theta(t)\right\} &+ V\mathbb{E}\left\{\sum_{i \in \mathcal{J}} C^\Pi(t)\right\} \\ &\leq B + VC_{p1}^*, \end{aligned} \quad (46)$$

where (44) and (45) in Lemma 1 have been used. Taking an expectation over $\Theta(t)$ on both sides and summing over $t \in \{0, 1, 2, \dots, T-1\}$, we obtain

$$V \sum_{t=0}^{T-1} \mathbb{E}\{C_{p4}^*(t)\} \leq TB + TVC_{p1}^* - \mathbb{E}\{L(\Theta(T-1)) - L(\Theta(0))\}. \quad (47)$$

Dividing both sides by TV yields:

$$\frac{1}{T} \sum_{t=0}^{T-1} \mathbb{E}\{C_{p4}^*(t)\} \leq \frac{B}{V} + C_{p1}^* - \frac{\mathbb{E}\{L(\Theta(T-1)) - L(\Theta(0))\}}{VT}. \quad (48)$$

Since $\mathbb{E}\{L(\Theta(T-1))\}$ and $\mathbb{E}\{L(\Theta(0))\}$ are finite, taking limits over T to infinity gives:

$$\lim_{T \rightarrow \infty} \frac{1}{T} \sum_{t=0}^{T-1} \mathbb{E}\{C_{p4}^*(t)\} \leq \frac{B}{V} + C_{p1}^*. \quad (49)$$

References

- [1] R.G. Charles, M. Davies, P. Douglas, I.L. Hallin, I. Mabbett, Sustainable Energy Storage for Solar Home Systems in Rural Sub-Saharan Africa – A Comparative Examination of Lifecycle Aspects of Battery Technologies for Circular Economy, With Emphasis on The South African Context, *Energy* 166 (Jan 2019) 1207–1215.
- [2] J. Aghaei, M.I. Alizadeh, Demand response in smart electricity grids equipped with renewable energy sources: a review, *Renewable and Sustainable Energy Reviews* 18 (2013) 64–72.
- [3] R. Deng, Z. Yang, M. Chow, J. Chen, A survey on demand response in smart grids: mathematical models and approaches, *IEEE Transactions on Industrial Informatics* 11 (3) (2015) 570–582.
- [4] J. Eyer, G. Corey, Energy Storage for the Electricity Grid: Benefits and Market Potential Assessment Guide, Sandia Report SAND2010-0815, Feb 2010.
- [5] X. Luo, J. Wang, M. Dooner, J. Clarke, Overview of current development in electrical energy storage technologies and the application potential in power system operation, *Applied Energy* 137 (Jan 2015) 511–536.
- [6] P.M. van de Ven, N. Hegde, L. Massouliè, T. Salonidis, Optimal Control of End-User Energy Storage, *IEEE Transactions on Smart Grid* 4 (2) (2013) 789–797.
- [7] Y. Xu, L. Tong, Optimal operation and economic value of energy storage at consumer locations, *IEEE Transactions on Automatic Control* 62 (2) (2017) 792–807.
- [8] Z. Wang, C. Gu, F. Li, P. Bale, H. Sun, Active demand response using shared energy storage for household energy management, *IEEE Transactions on Smart Grid* 4 (4) (2013) 1888–1897.

- [9] K. Paridari, A. Parisio, H. Sandberg, K.H. Johansson, Demand Response for Aggregated Residential Consumers with Energy Storage Sharing, in: *Proceedings of the 54th IEEE International Conference on Decision and Control (CDC)*, Osaka, Japan, Dec 15–18 2015, pp. 2024–2030.
- [10] W. Tushar, B. Chai, C. Yuen, S. Huang, D.B. Smith, H.V. Poor, Z. Yang, Energy storage sharing in smart grid: a modified auction based approach, *IEEE Transactions on Smart Grid* 4 (2) (2013) 866–876.
- [11] L. Gkatzikis, I. Koutsopoulos, T. Salonidis, The role of aggregators in smart grid demand response markets, *IEEE Journal on Selected Areas in Communications* 31 (7) (2013) 1247–1257.
- [12] W. Tushar, J.A. Zhang, D. Smith, H.V. Poor, S. Thièbaux, Prioritizing consumers in smart grid: a game theoretic approach, *IEEE Transactions on Smart Grid* 5 (3) (2014) 1429–1438.
- [13] W. Tushar, B. Chai, C. Yuen, S. Huang, D.B. Smith, H.V. Poor, Z. Yang, Energy storage sharing in smart grid: a modified auction based approach, *IEEE Transactions on Smart Grid* 7 (3) (2016) 1462–1475.
- [14] T. AlSkaf, A.C. Luna, M.G. Zapata, J.M. Guerrero, B. Bellalta, Reputation-based joint scheduling of households appliances and storage in a microgrid with a shared battery, *Energy and Buildings* 138 (2017) 228–239.
- [15] J. Yao, P. Venkatasubramaniam, Optimal end user energy storage sharing in demand response, in: *Proceedings of the 2015 IEEE International Conference on Smart Grid Communications*, Miami, Florida, USA, 2–5, Nov 2015, pp. 175–180.
- [16] Z. Huang, T. Zhu, Y. Gu, D. Irwin, A. Mishra, P. Shenoy, Minimizing electricity costs by sharing energy in sustainable microgrids, in: *Proceedings of 1st ACM Conference on Embedded Systems for Energy-Efficient Buildings*, Memphis, USA, Nov 5–6 2014, pp. 120–129.
- [17] I. Atzeni, L.G. Ordóñez, G. Scutari, D.P. Palomar, J.R. Fonollosa, Demand-side management via distributed energy generation and storage optimization, *IEEE Transactions on Smart Grid* 4 (2) (2013) 866–876.
- [18] D. Zhao, H. Wang, J. Huang, X. Lin, Pricing-based energy storage sharing and virtual capacity allocation, in: *Proceedings of the 2017 IEEE International Conference on Communications (ICC)*, Paris, France, 21–25, May 2017, pp. 1–6.
- [19] T.T. Kim, H. PoorKim, H. Poor, Scheduling power consumption with price uncertainty, *IEEE Transactions on Smart Grid* 2 (3) (2011) 519–527.
- [20] M. Puterman, *Markov Decision Processes: Discrete Stochastic Dynamic Programming*, Wiley-Interscience, 2005.
- [21] M. Neely, *Stochastic Network Optimization with Application to Communication and Queueing Systems*, Morgan & Claypool, 2010.
- [22] Y. Guo, M. Pan, Y. Fang, Optimal power management of residential customers in the smart grid, *IEEE Transactions on Parallel and Distributed System* 23 (9) (2012) 1593–1606.
- [23] S. Salinas, M. Li, P. Li, Y. Fu, Dynamic energy management for the smart grid with distributed energy resources, *IEEE Transactions on Smart Grid* 4 (4) (2013) 2139–2151.
- [24] S. Sun, M. Dong, B. Liang, Real-time power balancing in electric grids with distributed storage, *IEEE Journal of Selected Topics in Signal Processing* 8 (6) (2014) 1167–1181.
- [25] Y. Huang, S. Mao, R. Nelms, Adaptive electricity scheduling in microgrids, *IEEE Transactions on Smart Grid* 5 (1) (2014) 270–281.
- [26] W. Shi, N. Li, C. Chu, R. Gadh, Real-time energy management in microgrids, *IEEE Transactions on Smart Grid* 8 (8) (2017) 228–238.
- [27] S. Sun, M. Dong, B. Liang, Joint supply, demand and energy storage management towards microgrid cost minimization, in: *Proceedings of the 2014 IEEE International Conference on Smart Grid Communications (SmartGridComm)*, Venice, Italy, 3–6 Nov 2014.
- [28] S. Han, S. Han, K. Sezaki, Economic assessment on V2G frequency regulation regarding the battery degradation, in: *Proceedings of the third IEEE PES Conference on Innovative Smart Grid Technologies (ISGT 2012)*, Washington, DC, USA, 16–20 Jan 2012.
- [29] R. Urgaonkar, B. Urgaonkar, M. Neely, A. Sivasubramaniam, Optimal power cost management using stored energy in data centers, in: *Proceedings of the ACM SIGMETRICS joint International Conference on Measurement and Modeling of Computer Systems (ACM SIGMETRICS'11)*, San Jose, California, USA, 7–11, Jun 2011, pp. 221–232.
- [30] M. Grant, S.P. Boyd, CVX: Matlab software for disciplined convex programming, version 2.1. [Online]. Available: <http://cvxr.com/cvx/>.